Structural integrity assessment of self-elevating units with fatigue and corrosion damage based on actual load history

Master of Science Thesis

S.P.T. Berbers

TU Delft

Structural integrity assessment of self-elevating units with fatigue and corrosion damage based on actual load history

Master of Science Thesis

For the degree of Master of Science in Offshore Engineering at
Delft University of Technology

S. Berbers

September 05, 2017

Faculty of Civil Engineering and Geosciences,
Delft University of Technology

TU Delft

The work in this thesis was supported by Seafox.

Abstract

Seafox owns and operates a fleet of 12 Jack-ups. The design life of these Jack-ups is typically around 30 years. However, some have remained operational after exceeding their design life. It is therefore critical to gain an understanding how long and under what conditions these jacks-ups are still able to operate safely.

There are two main deterioration processes in Jack-ups as they age: metal fatigue and corrosion. Fatigue is a process that weakens material due to repetitive loading and unloading. Corrosion is the deterioration of a metal caused by an electrochemical reaction between it and its environment. In this thesis these two deterioration processes are assessed and quantified in two Seafox Jack-ups. Fatigue is assessed on the Seafox 2 and corrosion on the Seafox Burj.

The structural characteristics of a Jack-up result in a significant dynamic response. Therefore, a dynamic analysis is conducted to determine the stresses in the jack-up legs. Furthermore, various non-linearities justify a time domain finite element analyses conducted in USFOS. The thesis presents a structural model of the Seafox 2 using a simplified hull and spring elements to represent the hull-leg and leg-ground connections. Environmental loading is determined by using the actual wave records kept for each operating location of the Seafox 2 in a simulation. The simulation identifies a critical joint with the highest stress range. The hot spot stress range in this joint is determined using stress concentration factors (SCF), using two methods: parametric equations of Efthymiou and finite element analyses. From the hot spot stress ranges and the number of recorded stress cycles at each location the fatigue life of this critical joint is calculated with a S-N curve.

The critical joint is used as proxy to establish the design fatigue life of the Seafox 2 based on actual wave loading. The analysis shows a design fatigue life of the Seafox 2 of 262,2 years. This supports the conclusion that the rig can remain operational. Although the analysis conducted is a conservative one, the non-linearity of the S-N curve (small fluctuations in in stress cause large changes in fatigue life) makes it advisable to continue to check critical joints for cracks when the Seafox 2 is docked.

The Seafox Burj went into docking in 2015. Ultrasonic thickness measurements made it clear that the Burj had significant steel diminution due to corrosion in the legs. For commercial reasons Seafox wanted to know whether the legs needed to be replaced unconditionally, or that the Burj could still operate in lower water depths.

The ultimate limit state for the Burj, with steel diminution due to corrosion, is calculated for three locations. Two are possible locations where the Burj might be

deployed and one chosen as a model benchmark. The Burj is modelled in the same manner as the Seafox 2. From the results it can be concluded that steel diminution has a considerable impact on the ultimate limit state. The analysis indicates that the Burj, cannot operate in deep waters anymore without costly leg repairs. The analysis indicates that it can still operate safely in shallow waters. Therefore, narrowing the work scope of the Burj to shallower waters is a viable way to avoid costly leg repairs.

Acknowledgements

Contents

1 Introduction

A Jack-up rig or a self-elevating unit is a type of mobile platform that consists of a buoyant hull fitted with a number of movable legs capable of raising its hull over the surface of the sea. The buoyant hull enables transportation of the unit and all attached machinery. Once on location legs are lowered and the hull is raised to the required elevation above the sea surface. The Jack-ups support on the sea bed has the great benefit that it does not experience heave, pitch or roll. This greatly increases its operability. The first Jack-up was built in 1954 and rigs of this type have since been common solution for offshore drilling, turbine installation and offshore support.

The field work for this thesis was conducted at Seafox Group. Seafox owns and operates a fleet of 12 Jack-ups. Its main areas of expertise are offshore accommodation and crane support, well testing and workovers, and transportation, installation and decommissioning.

1.1 Problem definition

The design life of a Jack-up is typically around 25 years. However a large number have exceeded their design life and remain operational beyond this period. Indeed, in some cases, the operational life far exceeds the design life. Seafox still operates a number of Jack-ups built in the 1970's and 1980's, surpassing their design life by up to 22 years. As these Jack-ups remain in operation, they continue to deteriorate. It is therefore critical to gain an understanding of the different deterioration processes to ensure safe operation.

There are two main deterioration processes in a Jack-up as they age: metal fatigue and corrosion. Fatigue is a process where material weakens due to repetitive loading and unloading. These dynamic stresses can be much less in magnitude than what would cause yielding of the material in a single stress cycle. Corrosion is the deterioration of a metal that results from an electrochemical reaction with its surrounding environment. It creates byproducts commonly referred to as rust and causes diminution of the steel. This thesis assesses and quantifies metal fatigue in one and corrosion in another Seafox Jack-up.

The initial scope of the research was limited to the influence of fatigue damage on Jack-ups, using field data from the Seafox 2.. During the research one of the Jack-ups in the Seafox fleet (the Burj) came off contract and was brought into dry-dock for maintenance. Ultrasonic thickness measurement (UTM) revealed that significant steel diminution had taken place. For commercial reasons Seafox wanted to know if the legs needed to be replaced unconditionally or if it could still operate in lower water depths. Therefore the research was expanded to include corrosion effects and the interaction between corrosion and metal fatigue. This research into the effect of steel diminution on the ultimate limit state of a Jack-up has immediate commercial purpose.

1.2 Research objectives

The main research objective is to assess the structural integrity of the Seafox 2 with fatigue damage and the Burj with corrosion damage based on actual load history.
The thesis is structured to achieve the following objectives

1. Determine the fatigue life of the Seafox 2 (fatigue limit state).
2. Determine an accurate way to model environmental loading from different operating locations.
3. Determine what modelling considerations impact the fatigue life.
4. Determine the new ultimate limit state of the Burj with steel diminution.
5. Determine if it is possible to narrow the work scope for a Jack-up with corrosion damage.
6. Determine the influence of diminution on the fatigue life of the Seafox 2.

Thesis scope

This thesis focuses on the structural aspects of the legs of in-situ Jack-ups. This thesis excludes detailed analyses of soil mechanics that occur at the structures foundations, fatigue and corrosion damage in the hull and other structural components, and all aspects of the afloat situation. The latter is a maritime engineering topic.

1.3 Thesis structure

Chapter 2 gives an introduction into fatigue and its historical background. It presents two approaches for assessing fatigue damage: the S-N curve approach and the fracture mechanics approach. Both are elaborated and different ways for determining the stress concentration factor are discussed.

Chapter 3 describes modeling of a Jack-up structure in theory. It discusses the quasi-static and dynamic approach and evaluates the adequacy of the two approaches to describe the reality of a Jack-up. The different methods for conducting a dynamic analysis are addressed and the time domain finite element method is elaborated.

Chapter 4 describes the structural model of the Seafox 2. The chapter describes how the hull and legs are modelled and discusses the hull-leg interface and legs-to-ground interface. The chapter also discusses the environmental conditions for each location in which the Seafox 2 has operated.

Chapter 5 describes how a number of environmental simplifications are made to reduce the model size. The Chapter presents a finite element analysis to determine the stress ranges are determined. It also discusses the stress concentration factor (SCF)of a joint using two methods: parametric equations of Efthymiou and a new finite element model. After the stress ranges and SCF's are calculated the result on fatigue life are given.

Chapter 6 discusses the basics of corrosion and presents a structural model for the Burj. As in chapter 4, the hull and legs are modelled and the hull-leg interface and legs to ground interface are discussed. It also presents the environmental conditions for a 100 year storm in three different locations.

Chapter 7 presents evidence of the influence of diminution on the tolerable survival conditions in three locations. These three scenarios are in shallow-, intermediate- and deep water depth. Model runs using a number of diminution stages plot the stress increase in the members as a result of diminution. Unity checks are done for the critical members for each diminution stage.

Figure 1-1 shows the analyses setup in this thesis. It shows that fatigue damage and corrosion damage are in principle different processes. It also shows that the two processes are modelled on two different Seafox Jack-ups (the Seafox 2 and the Burj). The analysis of each process starts by defining it (Fatigue: chapter 2 and corrosion: chapter 6). Then a structural model is built in a finite element program for both the Seafox 2 and the Burj (chapter 4 and 6). For the Burj, 10 structural models are built each with different wall thicknesses to accommodate steel diminution. For the Seafox 2 the model is run for a number of different environmental conditions (chapter 5) whilst the Burj model is run for 100 year storm conditions (chapter 7). The dynamic analyses determine the member stresses. And the resulting ultimate limit state for the Burj. For the Seafox 2 the member stresses are multiplied by a stress concentration factor and combined with the number of cycles to determine the fatigue limit state. Stress increase from diminution is then translated to the Seafox 2 as rule of them to determine the impact of diminution on fatigue life (chapter 8).

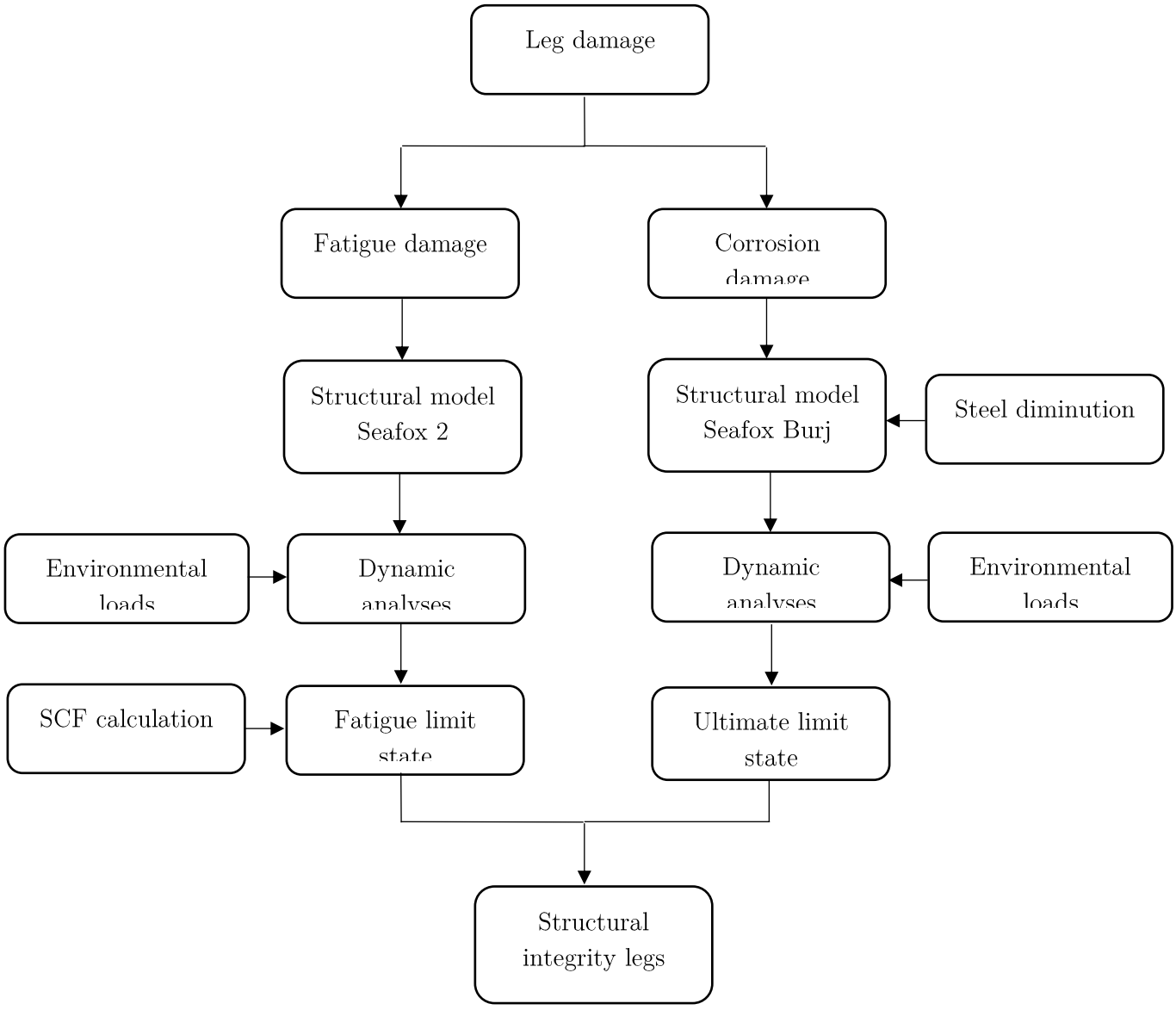

Figure 1-1 Analyses setup

2 Fatigue accumulation

Fatigue is a process where material weakens due to repetitive loading and unloading. These dynamic stresses can be smaller than what would cause yielding of the material in a single stress cycle. Fatigue is becoming a more and more important subject as the number of older structures increases offshore.

Section 3.1 gives an introduction into fatigue and presents a historical background. Section 3.2 presents two approaches for assessing fatigue damage: the S-N curve approach and the fracture mechanics approach. In section 3.4 different ways for determining the stress concentration factor are discussed, including a stress concentration factor to correct for geometric anomalies.

2.1 Introduction to fatigue

Fatigue damage not only occurs in the offshore industry but in all mechanical engineering sectors raging from the automotive-to the aviation industry. It was first properly studied and tested on railroad axles by August Wöhler in 1860. He concludes that cyclic stress range is more important than peak stress and introduces the concept of an endurance limit (Schutz, 1996). Since then the phenomenon has been extensively researched and different approaches have been established.

In essence fatigue is a process of damage accumulation initiated by yielding of a material through sliding of the atomic layers. This sliding is caused by a combination of dislocations and local stress concentrations. With each slip, however small, deteriorations occur in the materials structure (Sobczyk K., 1992). The dislocations increase in quantity with each stress cycle and link up to form plastic deformations. This is the start of a microscopic crack called nucleation (crack initiation). These microscopic cracks then grow in size and combine to form larger macro cracks and ultimately lead to failure of the material if the stress cycles continue.

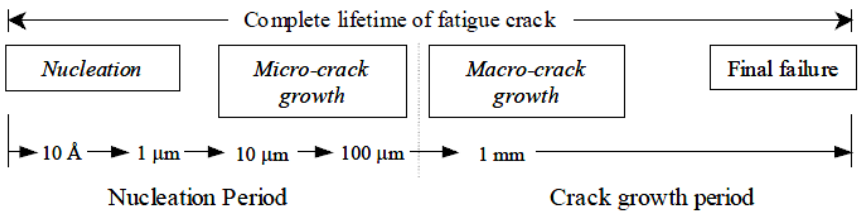

2.2 Fatigue assessment

The assessment of fatigue damage can be based on two approaches: fracture mechanics and the S-N curve approach.

2.2.1 Fracture mechanics

In the fracture mechanics approach a crack growth curve is established with a crack propagation law. The Paris-Erdogan law relate stress intensity factor to the crack growth rate per loading cycle (Paris P.C., 1963). The Paris' equation is used to predict the crack propagation or the fatigue life.

$$\frac{da}{dN} = C(\Delta K)^m$$

ΔK = *Stress intensity factor* ($K_{max} - K_{min}$)
N = *Number of cycles to failure*
a = *Crack depth.*
C, m = *Material parameters*

In Figure 2-1 an example of this relationship is given in which C and m are constants depended on the material.

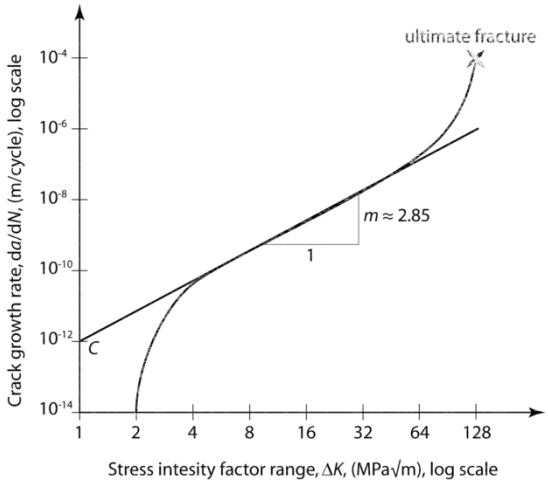

Figure 2-1 Relationship between crack growth rate and stress intensity factor

A major benefit of this method is that it takes the dimensions of the crack into account. Thus detection and measurement of a crack can serve as feedback input to calculate the limit state and to determine how much fatigue life is left in the material. Though this method describes the fundamentals of fatigue relatively accurate, major drawback is that it is based on single cracks (Collins, 1993). Therefore the analyses is mainly used in inspections. The method is predominately used for the crack growth period.

2.2.1.1 S-N curve approach

Second method is called the S-N curve approach which describes material failure after a certain amount of cycles. The foundations of this approach were laid by the earlier mentioned August Wöhler. He did a systematic and quantitative investigation on fatigue damage which resulted in the Wöhler curve or as we now know it the S-N curve (Schutz, 1996).

The S-N curve (Figure 2-2) displays fatigue data in the elastic stress range in a plot: nominal stress amplitude (S) versus number of cycles to failure (N). Data required for this plot is generated through numerous testing procedures for a single material. This gathered empirical data from the plot can then be used to calculate the design fatigue life. The method is predominately used to describe the crack nucleation period. Because in this thesis a fatigue life analysis is conducted, which includes the crack nucleation period, the S-N curve approach fits best. Fatigue damage accumulation and fatigue life will be elaborated on in the following sections

2.3 Damage accumulation

The stress amplitudes constantly vary as a consequence of dynamic loading from wind waves and currents. As S-N curves present results for constant stress amplitudes, standard S-N curves cannot be used directly in a situation with varying stress amplitudes. What is needed, therefore, is aa damage accumulation model.

2.3.1 Linear Damage (Palmgren-Miner rule)

Most commonly used damage model is the linear damage theory also known as the Palmgren-Miner rule. The theory states that the damage fraction at any stress level S_i is linearly proportional to the ratio of number of cycles to the total number of cycles that would produce failure at that stress level (Paris P.C., 1963).

$$D_i = \frac{n_i}{N_i}$$

That is if say: N_1 is number of cycles at which failure occurs and the stress amplitude is S_1 that occurs for a number of n_i smaller than N_1 will produce a smaller fraction of damage D_1.

When determining stress ranges from long-term irregular stress distributions, rainflow counting or peak counting can be used to determine a stress histogram. A stress histogram consists of a number of stress range blocks $\Delta\sigma_i$ each with a number of stress repetitions n_i.The fatigue criterion reads

$$D = \sum_{i=1}^{k} \frac{n_i}{N_i} = \frac{1}{\bar{a}} \sum_{i=1}^{k} n_i \cdot (\Delta\sigma_i)^m$$

D = *accumulated fatigue damage*

$\frac{1}{\bar{a}}$, m = *S-N fatigue parameters (Table 2-1 Parameters from S-N curve)*

k = *number of stress blocks*

n_i = *number of stress cycles in stress block i*
N_i = *number of cycles to failure at constant stress range* $\Delta\sigma i$

2.3.2 S-N curve

In this thesis, fatigue calculations are based on the S-N curve described by DNV-GL (DNVGL-RP-C203, 2016) for tubular joints.

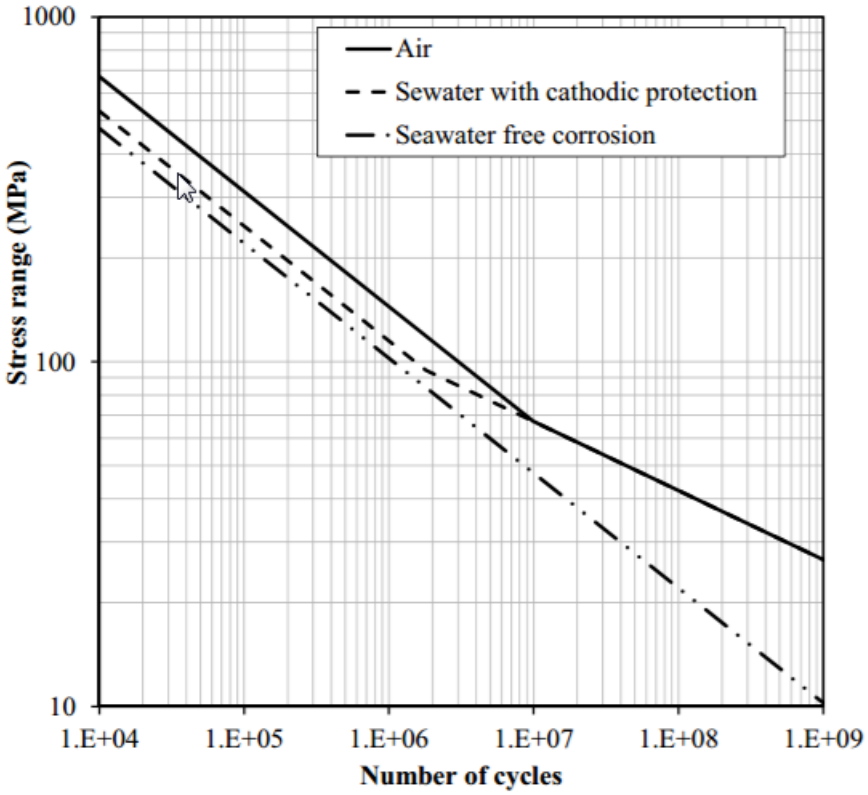

Figure 2-2 S-N curve for tubular joints (DNVGL-RP-C203)

In the S-N curve effects of a seawater environment are taken into account. S-N drops when the structure is subject to an corrosive environment and thus the fatigue life also drops.

Table 2-1 Parameters from S-N curve

Environment	m_1	$\log \bar{a}_1$	m_2	$\log \bar{a}_2$	*Fatigue limit at 10^7 cycles (MPa)*)*	*Thickness exponent k*
Air	N ≤ 10^7 cycles		N > 10^7 cycles			
	3.0	12.48	5.0	16.13	67.09	0.25
Seawater with cathodic protection	N ≤ $1.8 \cdot 10^6$ cycles		N > $1.8 \cdot 10^6$ cycles			
	3.0	12.18	5.0	16.13	67.09	0.25
Seawater free corrosion	3.0	12.03	3.0	12.03	0	0.25

2.4 Hot spot stress

To determine fatigue it is essential to understand there is a fundamental difference between nominal and hot spot stress. Nominal stress is the linear part of the stress distribution excluding joint geometry. Joint geometry can lead to stress build up. In critical areas where stress build up is high the term hot spot stress is used. To determine hot spot stress, the nominal stress must be multiplied by a stress concentration factor (SCF). These SCF's have major influence on the fatigue damage calculation and are therefore an essential part in determining fatigue life.

$$\sigma_{hot\ spot} = SCF\ \sigma_{nominal}$$

2.4.1 Parametric SCF formulae

A significant amount of research has been conducted on SCF calculation. This research indicates that parametric equations are an easy way of estimating the hot-spot stress in simple tubular joints.

Kuang (1975)

Kuang used a modified shell finite element program specifically designed to analyze tubular joints. It gives equations for T/Y, K and KT joint configurations. The tubular connections were modelled without a weld fillet, and stresses were measured at the mid-section of the member wall. The resulting stress estimates are therefore not very accurate.

Wordsworth and Smedley (1978 and 1981)

This work derives equations from acrylic model tests on tubular joints without a fillet weld. These equations tend to only give a good estimation for the chord side of a joint. (HSE, 1997)

Efthymiou and Durkin (1985 and 1988)

Efthymiou and Durkin published a series of parametric equations covering T/Y and gap/overlap K joints. Over 150 configurations were analyzed via a finite element program using 3-dimensional shell elements. The Efthymiou equations give a comprehensive coverage of all the parametric variations and are designed to be mean fit equations. They are also the standard in the DNV-GL guidelines and will be used in this thesis.

2.4.2 Numerical SCF calculation (FEA)

Finite element analysis can be used for the complete numerical calculation of the SCF's. Parametric equations give a good estimation on simple uni-planar joints but not always for more comprehensive multi-planar joints. For multi-planar tubular joints, such as in Jack-up legs, limited parametric and experimental information is available. These parametric equations are set with a certain validity range, thus requiring a finite element

model to be built for more complicated joints or when then the joints exceed the validity range.

This thesis uses both the parametric SCF formulae and a finite element and compares the different techniques for calculating stress concentration factors.

3 Modelling

Structures can be modeled as static, quasi-static and dynamic. In static problems the acceleration of a structure is assumed to be zero. When using a quasi-static approach the acceleration is assumed zero for any given instant in time. Effectively this approach assumes that structure deformations occur so slowly that inertia forces are very small and can be ignored. A dynamic analysis does not assume that acceleration is zero and takes inertia forces into account.

In this chapter both the quasi-static approach and the dynamic approach are discussed and the most suitable approach will be determined. In section 3.1 the quasi-static approach is explained and in 3.2 the dynamic approach. Then in section 3.3 the two approaches are evaluated on their adequacy to describe a Jack-up. Section 3.4 discusses the type of dynamic analyses in more detail.

3.1 Quasi-static approach

A quasi-static analyses is used to predict dynamic loading with a static equivalent. This can only be done when loading frequency is low compared to the natural frequency of the structure on which they are applied. The quasi-static approach assumes:

$$K\underline{x}(t) = \underline{F}(t)$$

This means the structures response is proportional to the loading or, in other words, that the response varies proportionally with the loading. It is important to note is that inertial loads are neglected in a quasi-static approach and this is also the methods major shortcoming.

Bottom founded Jack-ups are exposed to two principle forces: environmental forces acting predominantly in the horizontal direction and gravitational forces acting in the vertical direction. In this section these loads on a Jack-up are described.

3.1.1 Wind

Wind loads are caused by air particle hitting the structure and exerting a drag force. The magnitude of this force is determined by the shape of the structure and the particle velocity (wind speed).

$$f_{wind} = \frac{1}{2}\rho U^2 C_D A \tag{3-1}$$

In which U is the wind velocity, C_D the drag coefficient and A the area upon which the wind exerts force. The velocity profile of the wind varies depending on the height from sea level. To find the wind velocity at height z, the following relationship is used:

$$U = U_{ref}\left(\frac{Z}{Z_{ref}}\right)^{\alpha} \tag{3-2}$$

U_{ref} is defined by the 1-minute mean wind velocity at Z_{ref} at 10 m above MSL (mean sea-level). For open water a value of 0,1 is used for exponent α. As the wind velocity varies in height and the area of the structure may also vary in height it is common practice to divide the exposed areas into blocks. Each block is given a height and the wind force can then be calculated for each block separately. The total wind force is given by summation of all the individual blocks.

In this report wind loads on Jack-ups are modelled as static forces. Reason being that wind gusts tend to have a considerable longer period (30-240s) than the natural period of Jack-ups (<12s). (Tirant, 1993).

3.1.2 Wave and current loads

Both the Seafox 2 and the Burj have truss structured legs. The legs are comprised of chords and braces which have relatively small diameters compared to the wave length of incoming waves (recommended practice: $\lambda > 5$ D) (DNV-GL, 2015). The structure can therefore be considered slender and Morison's equation can be used (3-3). It states that if a structure is sufficient slender the particle velocities and accelerations in the direction normal to the member can be neglected.

Hydrodynamic loading can be calculated as a sum of an inertia force proportional to acceleration and a drag force proportional to the square of velocity.

$$F(t) = \frac{\pi}{4}\rho C_m D^2 U'(t) + \frac{1}{2}\rho C_D U(t)|U(t)| \tag{3-3}$$

C_m is the mass coefficient, which is the summation of the Froude-Krylov coefficient and a non-dimensional added mass coefficient C_a. $C_m = C_a + 1$. C_d is the drag coefficient, which is dependent on the shape of the structure, viscosity of the surrounding fluid, flow velocity and fluid density.

The particle velocity U and acceleration U' (derivative of velocity) can be calculated with several available wave theories. Two wave theories are relevant: the Airy wave theory and the Stokes 5th order wave theory. Wheeler stretching can be applied to the Airy wave theory to improve accurateness. The current velocity profile is simply superimposed

onto the wave velocity profile to give water particle velocities (and accelerations) across the depth profile.

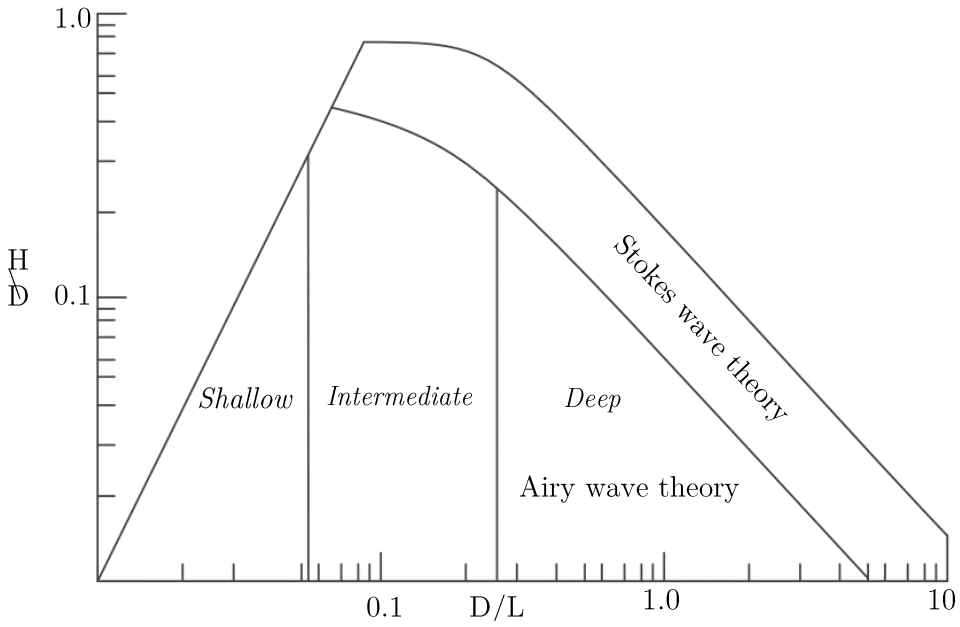

Figure 3-1 Validity of wave theories (for water depth D, wave length L and wave height H)

Airy wave theory (eq. (3-4 gives the horizontal velocity) gives a linearized description of the propagation of gravity waves on the surface of a homogeneous fluid layer.

$$u_a = \zeta_a \omega \frac{cosh(k\,(h+z))}{sinh(kh)} \sin(\omega t - kx) \tag{3-4}$$

In the extrapolated Airy wave theory wave crests, above mean sea level wave kinematics are assumed constant and equal to the value at z=0. To increase the accurateness of the Airy wave theory, wheeler stretching can be applied.

In the extrapolated Airy wave theory wave crests, above mean sea level wave kinematics are assumed constant equal to the value at z=0. To increase the accurateness of the Airy wave theory, wheeler stretching can be applied. Wheeler stretching is the process of extending linear Airy wave theory to points above the mean water level. This is achieved by substituting the vertical coordinate z with the scaled coordinate z (eq. (3-5)

$$z = (z - \eta)\frac{d}{d+\eta} \tag{3-5}$$

In which η is the surface elevation.

The magnitude in which the extrapolated- or stretched Airy wave theory differentiate depends on whether the waves on the structure are mass- or drag force dominated (inertia and drag part of the Morison equation) (Hydrodynamics, 2010). This dominance can be predicted by the Keulegan-Carpenter number K_C (eq. (3-6). For small Keulegan–Carpenter numbers inertia dominates, for large numbers the drag forces.

$$K_c = \frac{VT}{D} \tag{3-6}$$

In which V is the amplitude of the flow velocity, T the period of oscillation and D is the diameter of the structure. The Jack-up legs are truss structures with relatively small diameters. This results in a large K_C and therefore the researched Jack-ups can safely be assumed drag dominated.

To quantify the difference in the extrapolated- and stretched Airy theory and the Stokes 5th wave theory two simple beams are modeled in USFOS. One inertia dominated with a large diameter (5m) and one drag dominated with a small diameter (0,5m). An extrapolated-, stretched Airy and Stokes 5th wave is then modeled in USFOS (different wave theories can be selected in USFOS) to compare the wave force. The results are plotted in Figure 3-3 – 3.5.

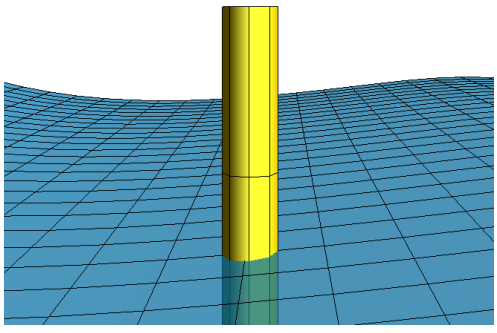

Figure 3-3 Inertia dominated structure

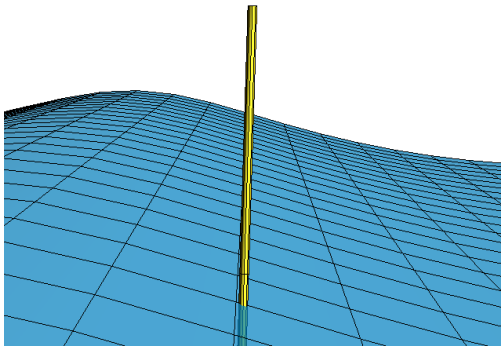

Figure 3-2 Drag dominated structure

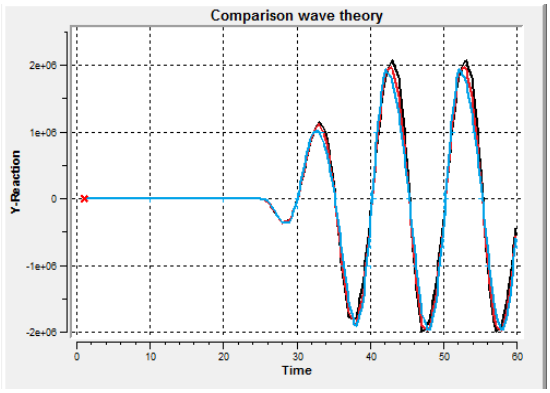

Figure 3-5 Inertia dominated, wave force vs time (black: stretched, red: extrapolated and blue: Stokes)

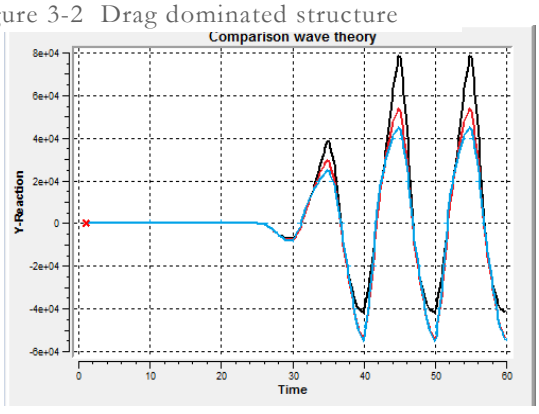

Figure 3-4 Drag dominated, wave force vs time (black: stretched, red: extrapolated and blue: Stokes)

3.2 Dynamic approach

A dynamic approach can be used to mitigate the shortcomings of the quasi-static approach (the quasi-static approach neglects inertia loads). This approach does not hypothesize that the structure is static at a given time. Different methods can be used to describe the dynamic response of a Jack-up. There are three primary methods of solving:

- SDOF Approach
- Frequency domain analysis
- Time domain analysis

3.2.1 SDOF Method

The Single Degree of Freedom (SDOF) method uses a mass- damper -spring system to model the Dynamic Amplification Factor (DAF) is defined as the ratio of the dynamic to the quasi-static response of a system:

$$DAF = \frac{x_{dyn}}{x_{stat}}$$

It is simply a dimensionless parameter that can be multiplied by the quasi static response in order to obtain the dynamic response for each different wave period. However by drastically simplifying the structure to a mass- damper- spring- system creates a number of errors, including:

Non-linear structural stiffness

The SDOF approach does not take into account the P delta effect and will thus care errors in the results. The SDOF approach models the stiffness of the structure as a linear spring. However, Jack-ups combine a large hull mass with relatively long, slender legs. They exhibit instances of the P-delta effect that occurs in structures that are axially loaded and have a horizontal deflection. Due to a deflection the structure will be eccentrically loaded and an additional moment will be created. This moment ($P \cdot \Delta$) will increase with a greater deflection and therefore the structure has a non-linear stiffness. . This is shown graphically in Figure 3-6, where P is the hull mass, V are environmental loads and Δ is the displacement. This effect is not taken into account in the SDOF approach and will therefore cause errors in the result.

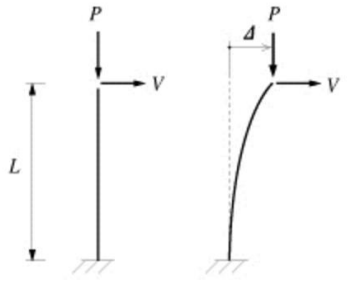

Figure 3-6 Schematization of the p-delta effect

Point mass

The SDOF approach models the weight of the structure as point mass. Whilst this might be possible for the hull, but not for the legs that also have a distributed mass. And added mass. In addition the added mass varies along the length of the legs. By modelling the leg and added mass as simply a point mass, one fictitiously increases the mass in the mass- damper- spring system. This, in turn, increases the natural period, thus causing errors.

3.2.2 Frequency domain analysis

Analysis in the frequency domain using discrete Fourier transformations can be used for calculating the dynamic response of linear systems. The frequency domain method involves linearization of the model and its loading before being solved deterministically (J.L. Humar, 1993). Frequency domain analysis is a robust method for solving dynamic problems. However when non-linearities are introduced the method becomes much more complex.

The Harmonic balancing method (HBM) is the most common way for solving non-linear dynamic response in the frequency domain. It is, however, rarely used in practical mechanics as the truncated Fourier expansion that HBM uses for frequency domain approximation of each degree of freedom (DOF) massively increases the total DOFs (O. Weeger, 2013). In addition commercial finite element analysis (FEA) software such as ANSYS, ABAQUS or USFOS (which is used in this thesis) do not calculate nonlinear frequency responses.

Non-linearity's in the Jack-up model include:

Structural stiffness

As described in 3.2.1 due to the P-Delta effect the structural stiffness of the Jack-up legs is non-linear.

Hydrodynamic drag

As described in 3.1.2, a Jack-up with trussed legs is drag dominated. The drag term in the Morison's equation varies non-linearly along the length of the leg. The effect of the non-linear drag term has been investigated by Pierson and Holmes, 1965, among others. Their analysis demonstrates how the probability distribution moves away from the Gaussian straight line to give much higher probabilities for high forces as the drag force becomes more dominant (Adams, 1991). The error becomes larger as the structure is more drag dominated., as illustrated in Figure 3-7.

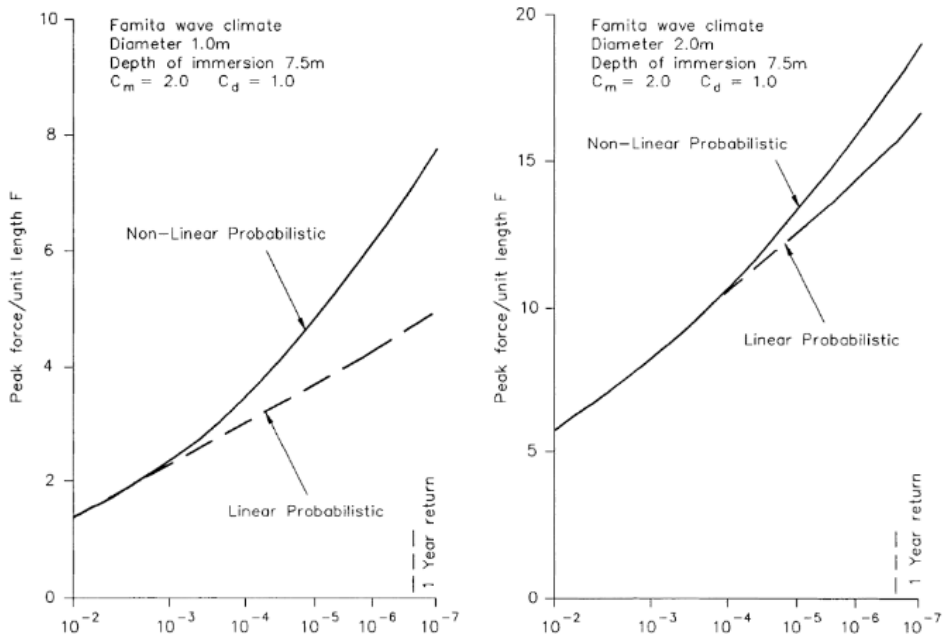

Figure 3-7 Long term probability distribution of peak force, member diameter 1,0m (left) and 2,0m (right). (Adams, 1991)

3.2.3 Time domain finite element analysis

The Finite Element Method (FEM) is a common method used for solving a variety of mathematical problems, including those posed by dynamic structural systems. FEM subdivides a structure into n elements, which are solved numerically to give an approximation of the solution for the complete system. Using FEM in the time domain allows for a complete description of the structure and all its nonlinearities. This is the reason FEM is often the preferred method for solving dynamic structures. A downside of the method is its need for lots of computational power for accurate approximations. This is increasingly obviated by the sharp increase in computational power of computers.

3.3 Quasi-static analyses or dynamic analyses

The eigenvalue analysis of the structural model indicates that the natural frequency (first mode of vibration) is 5,2 seconds. This frequency lies within the loading frequency spectrum. The fatigue limit state (FLS) calculation has to take into account all wave frequencies, including those with a wave frequency around 5,2 seconds. This means that resonance will take place and that inertial loading due to dynamic response cannot be neglected. To fully incorporate the dynamic response due to inertial loading it is advisable to use the dynamic approach.

A quasi-static approach can be used when determining the ultimate limit state (ULS), as long as the environmental loading frequency of a 100 year storm lies well outside the range of the natural frequency of the structure. This approach, however, neglects non-linearities and should be used with caution.

As discussed in section 4.2 the SDOF approach to solving structural dynamic problems does not include non-linear structural stiffness. This is a weakness for modelling Jack-ups that combine a large hull mass and relatively long, slender legs. In such cases, the P-Delta effect will have significant influence.

The frequency domain analysis approach to dynamic problems does not take the non-linearly varying hydrodynamic drag into account. As described in section 3.1.2 the trussed legs of Jack-ups are drag dominated and this feature cannot be neglected. The frequency domain analyses also does not take into account the non-linear structural stiffness.

Taking these facts into consideration the time domain finite element analyses is the best fit for the analysis at hand. The time domain FEA is discussed in the next section.

3.3.1 USFOS

USFOS is a finite element software package to simulate the behavior of space frame offshore structures under load. It is developed by SINTEF and the Norwegian University of Science and Technology through a joint industry project (USFOS Manual).

USFOS is used to perform strength calculations on structures through finite element analysis. The program uses one finite element per physical element of the structure, allowing the model to use the same finite element discretization as in linear, elastic analyses. The formulation includes nonlinear geometry and nonlinear material properties.

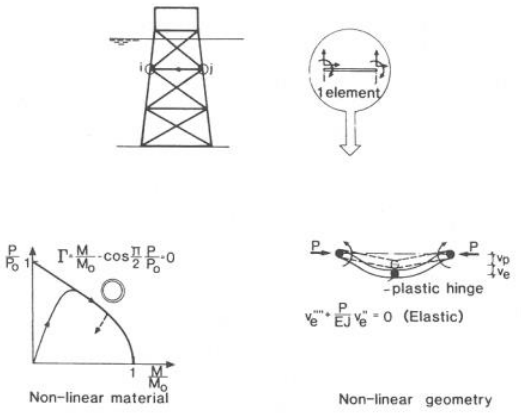

USFOS uses the updated Lagrangian approach to solve the discretization. In the updated Langrange formulation, the state variables are redifined (updated) at the end of each analysis increment. . So the current state is assumed to be the new refrence state. (Nagtegaal, 1982). In practice this means that the loads are applied in steps. For each one of these steps the system's stiffness equations are solved. At the end of each step all forces, moments, stress resultants, displacements etc. are updated and the process is repeated. Thus, each step constitutes a full, linear analysis, based on the updated information from all previous analysis steps.

4 Modeling the Seafox 2

This chapter describes how the hull and legs of the Seafox 2 are modelled and discusses the hull-leg and legs-to-ground interface. The chapter also discusses the environmental conditions for each location in which the Seafox 2 has operated.

4.1 The Seafox 2

The Seafox 2 is a four legged, non-selfpropelled, self-elevating accommodation unit (jack-up). It was designed by Marine Structure Consultants (MSC) and built by Cammell Laird Shipbuilders in 1985. It was acquired by Seafox (named Workfox at the time) in 2005. Its primary activity is to provide accommodation-, construction-, maintenance support and well services.

Figure 4-1 Seafox 2

The Seafox 2 is chosen to examine the influence of fatigue on the structural properties of the legs for a number of reasons:

- The Seafox 2 is sufficiently old to have acquired fatigue damage.
- The only fatigue study done on the Seafox 2 is a site specific one and conducted in 1983.

A fatigue damage investigation is also mandatory under DNV-GL guidelines . The Seafox fleet complies with DNV-GL regulations which since 2013 describe a mandatory fatigue analyses for rigs that are older than 15 years. This mandatory assessment has not yet been conducted for the Seafox 2.

4.2 Modeling the Seafox 2

For calculation of the stress cycles in the Seafox 2 legs the complete rig is modelled in 3D. This is done because of the various non-linearities associated with the dynamics of Jack-ups and the fact the natural frequency lies within the loading frequency of a fatigue limit state analyses (chapter 4). The model is build and run in USFOS (chapter 3.3.1).

4.2.1 Structural model

The process of modelling the Seafox 2 starts by building a structural file. From 2D CAD drawings (Appendix D) measurements are taken and nodes are created manually by assigning x-y-z coordinates. These coordinates are first listed in Excel and then imported into USFOS via text format. In total, a little under 3000 nodes with corresponding coordinates were created. From the nodes members are created. These consist of beam-, plate- and sub shell elements. The legs completely comprise of beam elements. Each beam element is assigned a geometry ID and a Material ID.

The model adds sub shell elements at high stress areas in the legs, This results in a smaller mesh size in high stress areas and thus increase the model's without drastically increasing the computation time associated with a smaller mesh size for the whole structure. Sub shells keep all the properties of the beam element it incases but allows the mesh size to be controlled independently. The hull is modelled with plate elements. Modelling is done according to (NEN-EN-ISO, 2012) guidelines.

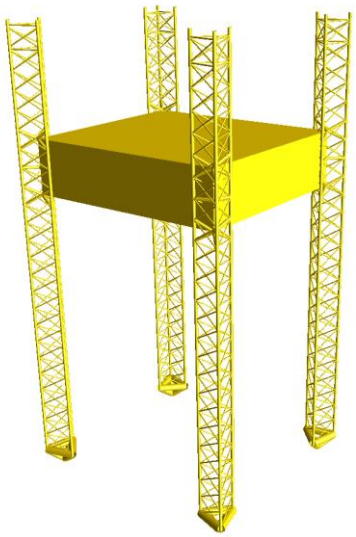

Figure 4-2 Structural model Seafox 2

4.2.2 Hull and legs

Hull

The complex hull structure with bulkheads, walls, girders, stiffeners etc. is simplified by using plate elements to form a box. The guidelines allow for this approach only if the structural properties of the hull as a whole are kept (NEN-EN-ISO, 2012). The latter are shown in Table 5-1.

Table 4-1 Structural properties hull

Elevated weight	G	5815000	[kg]
Torsional stiffness	I_x	15,0	[m^4]
Bending stiffness	I_y	3,01	[m^4]
Bending stiffness	I_z	65,1	[m^4]

The height and length of the modelled hull plates are equal to the dimensions of the actual hull but the width of the plates is adjusted to match the bending stiffness of the actual hull. Torsional stiffness is given by horizontal plates. The cross-sectional geometry of the horizontal plates is set to match the torsional stiffness of the actual hull. The elevated weight must be considered and simply adding point forces equal to the weight of the elevated hull will not suffice as the inertia effect would be ignored. Including inertia while keeping the geometries of the hull is accommodated by adjusting the density in the material properties of the modelled hull plates, thus adding mass across the whole structure

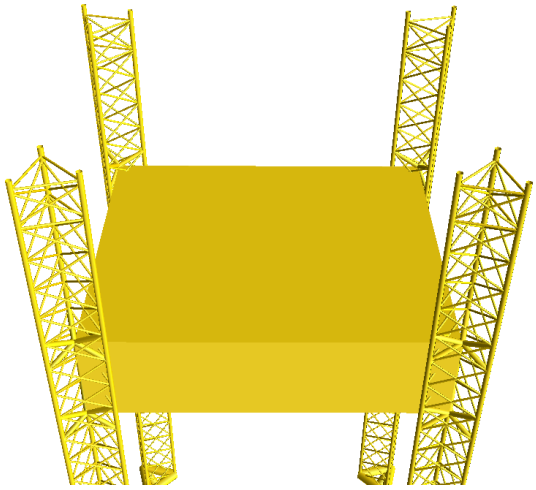

Figure 4-3 Modelled hull Seafox 2

Legs

The Seafox 2 truss legs consist of three chords interconnected by X-bracing. All the braces and chords are tubulars members with different diameters, thicknesses and yield strengths described in Table 4-2.

Table 4-2 Material properties Seafox 2 legs

Material ID	E-mod	poiss	yield	density	term.expansion
1	2.10E+11	0.300	4.50E+08	7.85E+03	0
2	2.10E+11	0.300	4.85E+08	7.85E+03	0
3	2.10E+11	0.300	5.55E+08	7.85E+03	0
4	2.10E+11	0.300	6.90E+09	7.85E+03	0

All members are all modelled in the structural file. Furthermore marine growth is added. The exact marine growth is unknown and the model uses NEN-EN-ISO 19905 standards of 12,5 mm (section *A.7.3.2.5*). This means a total of 25mm across the diameter of a tubular member. USFOS lets the user manually set the marine growth with the command M_GROWTH.

Table 4-3 Leg tubular geomerty

Geometry ID	D_o	t
1	0.24	0.025
2	0.60	0.07
4	1.6	0.75
5	0.6	0.28

Spudcans

When modelling the spudcans, rigid beam elements are considered sufficient to achieve an accurate transfer of the seabed reaction into the leg chords and bracing. (NEN-EN-ISO, 2012).

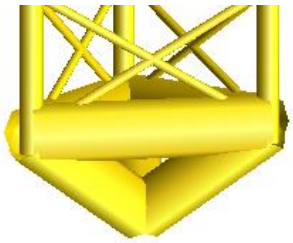

Figure 4-4 Modelled spudcan

4.2.3 Hull - leg interface

The Seafox 2 has a floating pin and hole jacking system (see Figure 4-5 Representation of a pin). The connection between the leg and hull is formed by an upper guide frame, a lower guide frame and jacking pins which slide in holes in the leg chords. Every chord has two holding pins and two jacking pins. During jacking the working- and the holding pins are inserted alternately. When the elevated height is reached only the holding pins are inserted. The holes in the chords are oversized to prevent the pins from sticking when retracted.

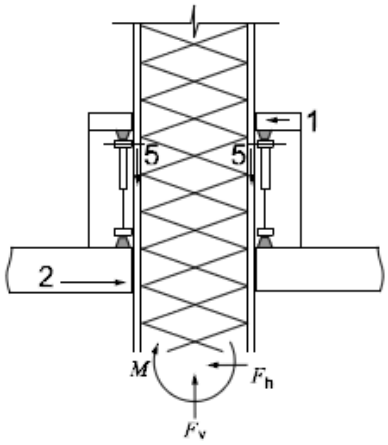

Figure 4-5 Representation of a pin and hole jacking system

There are three fundamental forces being transferred in the hull-leg connection: vertical forces, horizontal forces and a moment (Figure 4-5). Horizontal forces are all absorbed by the upper- and lower guide frames as the Seafox 2 has no fixation system like most modern Jack-ups and the floating pin and hole systems are designed for vertical forces only. Vertical forces are all transferred via the jacking pins. Because the holes in the chords are oversized in comparison to the jacking pins the connection can safely be assumed to be a pinned support and thus no moment is transferred by a single pin to a single hole. However, differences in vertical forces in opposing pins can create an internal moment in a chord. Because both pins are connected by a steel yolk (Figure 4-6) and thus cannot move up and down independently these internal moments are considered to be very small and are not taken into account.

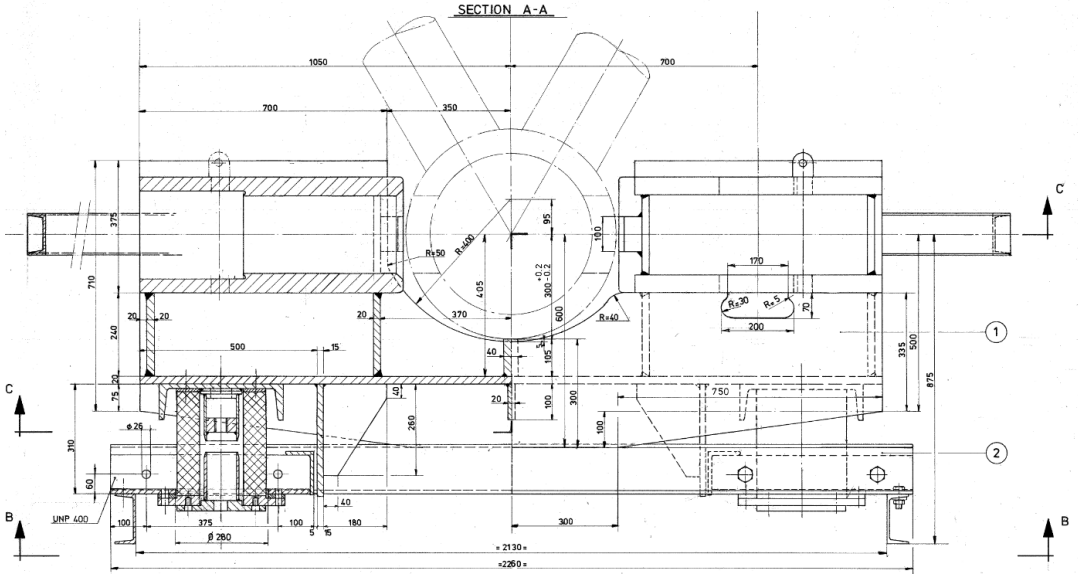

Figure 4-6 Top view of the pin and hole connection

The model represents the guide frames and jacking pins by rigid beams connecting the hull to the legs. The rigid beams are connected to the chords via springs. The spring stiffness's are discussed in the next section. The rigid beams are located at each end of the two guide frames circled in red in Figure 4-7. It is assumed that when the legs bend under load the load is transferred through these points. Furthermore, the holding pins are modelled by the beams in the middle. The beams connecting the hull to the legs is highlighted in pink in Figure 4-7.

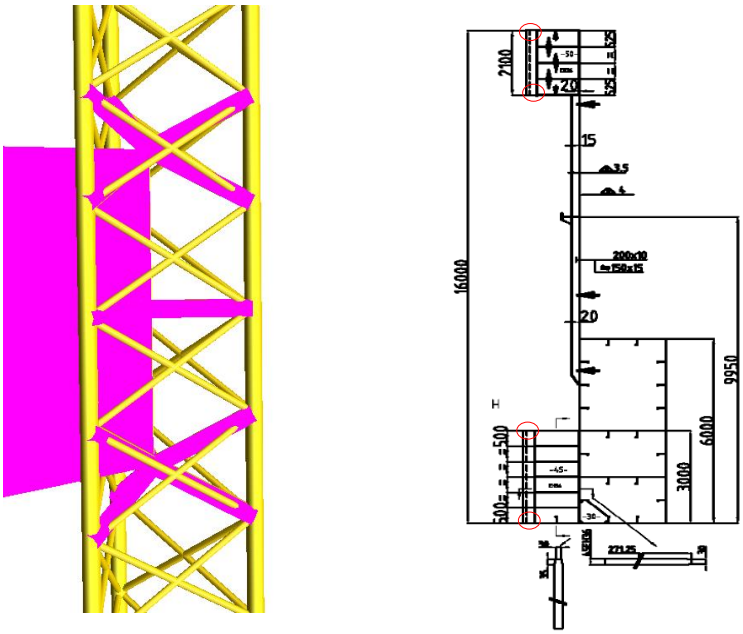

Figure 4-7 Highlighted modelled connecting rigid beam (left). Cross section of the jack house with connecting points circled in red (right)

Connecting spring stiffness

All modelled rigid beams are connected to the chords with 6 DOF springs. The modelled beams representing the upper and lower guide can only transfer forces in the horizontal plane. As the upper and lower guide plates consist of steel they are modelled rigid in the horizontal plane (Figure 4-8). As the chord is free to move up and down along the guide frame the vertical spring stiffness is very small. The vertical friction along the guide plates is neglected as is the little space between the guide frame and the chord. To summarize k_x and k_y are rigid and k_z, k_{rx}, k_{ry} and k_{rz} are almost zero.

Figure 4-8 Guide plate and leg chord

The modelled rigid beams in the centre of the hull (Figure 4-7 left) represent the jacking connection. As the Seafox 2 has a floating jacking system it is free to move in the horizontal plane. Hence the modelled spring connecting the rigid beams to the chords has a k_x and k_y of almost zero. The vertical stiffness of the spring depends on the structural stiffness of the holding pins (Figure 4-9) and the stiffness of the shock pads circled in red in Figure 4-10. The stiffness of the shock pads is taken from the Seafox 2 operating manual. The shock pads may degrade over time and become slightly stiffer, but this effect is not taken into account. The structural stiffness of the pins is determined by E, I and the length between the chord hole and the yoke holding the pin. The pin is considered with a fixed end end support in the yoke and thus $k_{z,pins}=3EI/l^3$. Summarized: k_x, k_y k_{rx}, k_{ry} and k_{rz} are almost zero and $1/k_z = 1/k_{z,pins} + 1/k_{shockpads}$.

Figure 4-9 Jacking pins

Figure 4-10 Holding pins inside the jack house

4.2.4 Leg - ground interface

Each of the four spudcans are connected to the ground by means of a spring. The spring has 6 degrees of motions as given in eq. (4-1).

$$\begin{bmatrix} F_x \\ F_y \\ F_z \\ M_x \\ M_y \\ M_z \end{bmatrix} = \begin{bmatrix} k_1 & & & & & \\ & k_2 & & & & \\ & & k_3 & & & \\ & & & k_4 & & \\ & & & & k_5 & \\ & & & & & k_6 \end{bmatrix} \begin{bmatrix} U_x \\ U_y \\ U_z \\ r_x \\ r_y \\ r_z \end{bmatrix} \tag{4-1}$$

The spring stiffness depends on the penetration depth of the spudcans and on the soil parameters. The stiffness in the horizontal plane (k_1, k_2) can be assumed high, as a considerable amount of force is needed to overcome soil- friction and pressure in this plane (no sliding is assumed to occur). Because Jack-up's are always preloaded when jacking the ground under the spudcans will compact. Therefore, k_3 can also be considered high. Rotation stiffness in the spring or ground fixity, has considerable effect on the model. The fixity can vary from none at all (pinned supports) to complete fixity (fixed supports).

Fixity

Soil conditions and penetration depth of the spudcans differ at each location, changing the fixity of the leg ends. A review of a number of SSAs (site specific assessments) does not support a conclusion on how to calculated fixity. Some SSAs express the fixity as a percentage between hinged- and fixed support and others give only a rotational spring stiffness. This study uses the conservative assumption that the rational spring stiffness's is completely pinned. When pinned supports are used all the bending moment stress must be absorbed by the leg guides, thus causing higher stresses in the legs at the height of the hull and larger deflections causing higher stress.

To check shear stress in the legs at the spudcans and confirm the assumption larger stresses occur in the legs with pinned supports, the model is also run with fixed supports. The stresses at the spudcan – leg transition are relatively low compared to stresses in the legs at guide frame. Also the assumption that stresses are higher when a pinned support are used deems to be correct. Thus using a pinned support will lead to higher stresses in the legs. The used spring stiffness: k_x k_y and k_z are rigid and k_{rx}, k_{ry} and k_{rz} are almost zero.

The leg fixity also influences the dynamics of a jack-up. Fixed supports will decrease the natural period of the Jack-up. A lower natural period will lead to resonance at lower wave heights. Lower waves contain less energy and exert less force on the structure. For the ultimate limit state this is considered favourable however, when a fatigue study is conducted one has to consider the fact that waves with a lower height occur more often.

The amount of stress cycles where resonance occurs will therefore increase. This can have a negative effect on the fatigue life.

Lower wave heights have a lower particle velocity. From Morison's equation it is known that a decrease in particle velocity in lower wave heights lead to a quadratic decrease in wave force. A lower wave force causes a decrease in stress range in the structure. A decrease in stress range from wave loading leads to a non-linear increase in fatigue life, with the same number of cycles.

Scatterplots are checked to quantify the number of waves with a lower natural period. The increase in the number of waves (and therefore stress cycles) with a lower period is deemed marginal. Therefore, the non-linear effect on fatigue life of a non-linear decrease in member stress is considered to have a larger effect on fatigue life than the increase in the number of stress cycles at the resonance frequency. Therefore the choice of pinned supports is considered conservative, however, the exact effect of fixity on dynamic behaviour needs more research.

4.2.5 Alternatives Considered

A computational model is a representation of reality and must not be mistaken for reality itself. The structural model of the Seafox 2 can be built in a variety of ways and this study tested a number of different configurations. These were evaluated against on the results of SSAs (Site Specific Assessment). These SSAs are quasi-static analyses to determine the ultimate limit state and do not include dynamic behaviour. However, as the loading frequency at the ultimate limit state lies sufficiently far from the natural frequency it is assumed accurate. Furthermore the natural frequency was benchmarked against the manufacturers manual. Different configurations that proved to not represent reality close enough are shown in figure Figure 4-11.

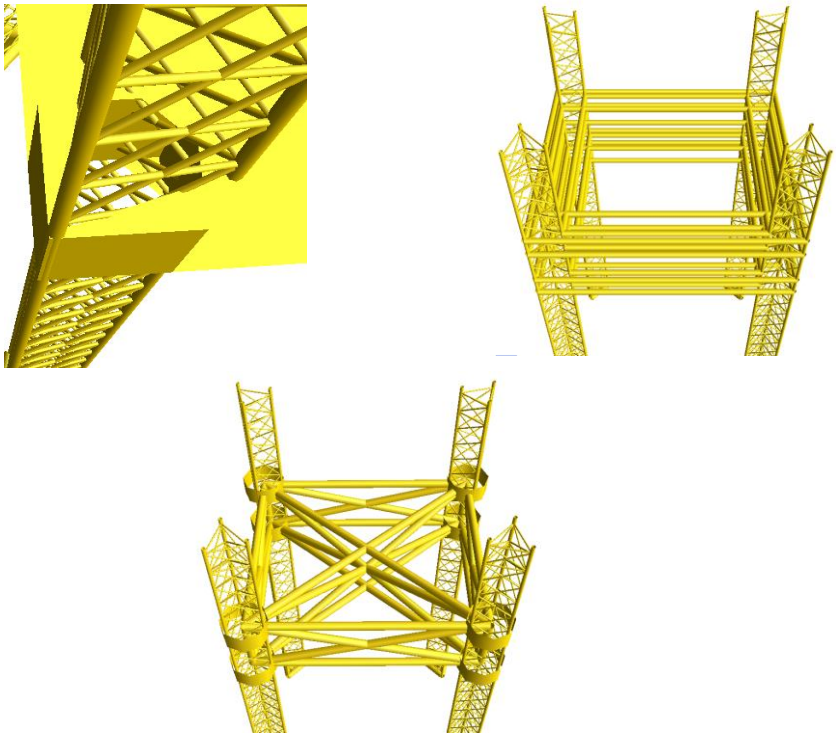

Figure 4-11 Clockwise: Complete plate connection, Beamed hull, Legs spatially locked in beam hull

4.3 Environmental conditions

Conventional fatigue analyses describe a predicted fatigue life based on expected stress cycles induced by environmental forces. The environmental conditions used are based on long-term averages in large regions. Scatterplots and wave spectra are used to predict future wave conditions at a certain given location. These industry standards are accurate for fixed platforms as they stay on the same location during their lifetime but Jack-ups move around and thus encounter a variety of different environmental conditions. This study uses measured environmental data from previous locations where the Seafox 2 has operated (hindcasting) for the determination of fatigue accumulation. Archival research yielded wave heights, wave periods, wave directions, wind speeds, wind directions, current- speeds and directions for all locations the rig has operated except one. Using measured environmentals as compared to average one will give a more accurate image into the fatigue state of the Seafox 2. This approach can then be compared to conventional methods.

4.3.1 Location history

First a database is built for all past locations and the number of days at each location. The complete database is found in appendix A.1. The number of days at each location is summarized in Table 4-4.

Table 4-4 Number of days at each location

Location	days
F15	250
K5	1198
K6	1287
L4	192
L7	297
K4	71
Leman	1109
Barque	180
Morecambe bay	1506
AK-A (GoM)	1315
Nohoch (GoM)	729

4.3.2 Wave heights

For each location wave records are gathered. Example records from the Leman field are shown in Table 4-4-5. The mean waves per day per wave block are then multiplied by the number of days at the specific location. The next chapter elaborates on the assumptions made.

Table 4-4-5 Number of waves at Leman assigned to wave height and direction

Wave Height (m)	N	NE	E	SE	S	SW	W	NW	All	per day per wind direction
0,50	427910	294757	276692	184114	222293	527582	370042	335153	2638543	903,6106
0.50:1.00	355249	202791	202897	135763	165560	474921	344916	306828	2188925	749,6318
1.00:1.50	149854	71792	77037	49296	71004	248013	190072	151278	1008346	345,324
1,50: 2.00	61995	29131	32705	19996	34913	133707	105087	75822	493356	168,9575
2.00:2.50	26326	12841	14804	8394	17730	72768	57368	38038	248269	85,02363
2.50:3.00	12039	6227	7068	3569	9008	40011	31434	19488	128844	44,12466
3.00: 3.50	5847	3245	3414	1468	4486	21917	17377	10231	67985	23,28253
3.50:4.00	3004	1772	1632	568	2190	11884	9752	5538	36340	12,44521
4.00: 4.50	1621	986	765	204	1052	6360	5569	3094	19651	6,729795
4.50: 5.00	910	548	350	68	497	3361	3232	1779	10745	3,679795
5.00: 5.50	526	301	157	22	231	1756	1899	1048	5940	2,034247
5.50: 6.00	310	161	68	7	105	909	1122	627	3309	1,133219
6.00: 6.50	185	84	29	2	47	467	664	378	1856	0,635616
6.50:7.00	112	43	12	1	20	239	391	228	1046	0,358219
7.00: 7.50	68	21	5	0	8	123	230	137	592	0,20274
7.50:8.00	42	10	2	0	3	63	134	81	335	0,114726
8.00: 8.50	26	5	1	0	1	33	77	48	191	0,065411
8.50: 9.00	16	2	0	.	0	18	45	28	109	0,037329
9.00: 9.50	10	1	0	.	0	9	26	16	62	0,021233
9.50:10.00	6	0	0	.	0	5	14	9	34	0,011644
10.00:10.50	4	0	0	.	0	3	8	5	20	0,006849
10.50:11.00	2	0		.	0	2	5	3	12	0,00411
11.00:11.50	1	0		.	.	1	3	2	7	0,002397
> 11.50	2	0	.	.		0	2	1	5	0,001712
Total	1046066	624717	617636	403472	529149	1544154	1139468	949858	5715052	1957,21

A mean period is calculated per wave height block from the scatter diagram. For example at the Leman field the wave range is 2 to 3 meters and has an average period of 5,9 s. These wave periods are then averaged for all locations. The next chapter elaborates on the assumptions made..

Table 4-6 Scatter diagram Leman field

		LEMAN																						
		Individual Wave Period [seconds]																						
Individual Wave Height [metres]	Min / Max	0	1	2	3	4	5	6	7	8	9	10	11	12	13	140	15	16	17	18	19	200	210	220
		1	2	3	4	5	6	7	8	9	10	11	12	13	14	15	16	17	18	19	20	21	220	230
9.0	10.0																							
8.0	9.0									1	1	1												
7.0	8.0							1	4	3	2	1												
6.0	7.0							11	39	27	8	5	3											
5.0	6.0						15	157	224	135	56	22	9	5	1									
4.0	5.0					4	262	1352	1488	717	264	117	52	19	8	4	1	1						
3.0	4.0				4	260	4366	1.0e4	8491	3700	1384	515	215	85	40	17	7	3	2					
2.0	3.0			17	443	1.2e4	5.2e4	6.2e4	4.0e4	1.7e4	6339	2225	820	294	103	35	17	6	3	1				
1.0	2.0		79	5555	7.2e4	2.8e5	3.7e5	2.7e5	1.5e5	5.9e4	2.1e4	7345	2497	864	310	86	29	11	4	2				
.0	1.0	9.8e4	4.5e5	9.9e5	1.4e6	1.3e6	7.8e5	3.9e5	1.7e5	6.3e4	2.2e4	7921	2863	1034	399	165	70	30	14	8	4	1	1	
Sum		9.8e4	4.5e5	1.0e6	1.5e6	1.6e6	1.2e6	7.4e5	3.6e5	1.4e5	5.2e4	1.8e4	6459	2301	861	307	124	51	23	11	4	1	1	0

Table 4-7 Total number of waves in each wave block

wave range	L4	L7	K4	K6	F15	K5	Leman	Braque	Morecambe bay	AK-A (GoM)	Nohoch (GoM)	Total per wave direction	Total cycles
0,00: 1,00	317423	514143	112198	2130204	390807	1991923	514143	263287	1991923	2126849	263287	10616187	84929494
1,00: 1,51	98742	147737	36317	661010	133198	612308	147737	93799	612308	455753	93799	3092710	24741681

1,51: 2,06	78994	118190	29054	528808	106559	489846	118190	75040	489846	364603	75040	2474168	19793344
2,06: 3,00	24796	35008	9064	165339	35603	152098	35008	42653	152098	72161	42653	766480	6131841
3,00: 4,00	6860	9163	2529	45807	10405	42189	9163	6519	42189	11014	6519	192356	1538844
4,00: 5,00	1999	2565	753	13406	3245	12467	2565	1873	12467	1629	1873	54841	438728
5,00: 6,00	608	762	235	4089	1062	3863	762	580	3863	237	580	16643	133142
6,00: 7,00	191	235	76	1280	357	1227	235	184	1227	35	184	5231	41847
7,00: 8,00	61	73	24	405	122	391	73	59	391	4	59	1664	13309
8,00: 9,00	20	23	8	128	43	125	23	19	125	1	19	532	4256
9,00: 10,00	6	7	3	41	15	40	7	1	40	1	1	162	1295
10,00: 11,00	2	2	1	14	6	12	2	0	12	0	0	50	403
11,00: 12,00	1	1	0	5	2	5	1	0	5	0	0	20	163
12<	0	0	0	0	1	0	0	0	1	0	0	2	16

4.3.3 Wind force calculation

Wind force is determined by dividing the Seafox 2 into a number of area blocks. For each area block the area is then calculated from CAD drawings. This is done for 180, 225 and 270 degrees. The wind force is then calculated with Eq. 4.3. At 225 degrees the wind force is highest as is shown in Table 4-4-8. The other directions are found in appendix A.3.

Eq. 5.3

$$f_{wind} = \frac{1}{2}\rho U^2 C_D A$$

Table 4-4-8 Windforce at 225 degrees

Direction	225				
Hull	67,3	6	0	1	1,11E+05
Jacking structure	18	10	6	1	4,96E+04
Accomodation	48,8	18	6	1	2,42E+05
Helideck	26	1	24	1	7,17E+03
Life boats	10	3	20	1	8,27E+03
Crane boom	2,5	40	8	0,5	1,38E+04
Crane pedestal	2,6	15	6	1	1,07E+04
Crane house	6	4	6	1	6,62E+03
Equipment on deck	5	3	6	1	4,13E+03
Funnel	4	6	6	1	6,62E+03
Crane house 2	3	5	21	1	4,13E+03
Crane boom 2	27,5	3,5	25	0,5	1,33E+04
Total					4,78E+05

4.3.4 Summary of the modelling considerations

Crack propagation	S-N	The S-N curve approach best describes the crack nucleation period.
Stochastic	Deterministic	Because actual environmental data is available a deterministic approach is chosen.
Stretched/extrapolated Airy	Stokes 5th	For the related depth and wave length, Stokes 5th describes the waves best.
Drag dominated	Inertia dominated	From the analyses done in section 3.1.2 it can be concluded the jack-up legs are drag dominated.
Pinned supports	Fixed supports	Pinned supports result in a higher stress range in the legs and is the most conservative choice. This effect is deemed to have a larger effect on fatigue life than the increase in stress cycles at resonance frequency.
Quasi static	Dynamic	The structural characteristics of a Jack-up result in a dynamic response. Therefore inertia loads cannot be neglected.
Linear	Non-linear	Due to non-linear structural stiffness and hydrodynamic drag a non-linear analyses is conducted.
Time domain	Frequency domain	Because of the Jack-up non-linearities a time domain analyses is conducted.

5 Fatigue life calculation

This chapter presents the Seafox 2finite element model results, using a number of environmental simplifications to reduce the model size. The finite element analysis determines the stress ranges for each wave block. To calculate the fatigue life of the structure a critical joint, which shows the highest stress range, is used as proxy. The stress range in the critical joint is multiplied by stress concentration factors (SCF's). These are derived using two: parametric equations of Efthymiou and a new finite element model for a joint. Finally, the stress ranges and SCF's are used to calculate the resulting fatigue life.

5.1 Stress calculation

The previous chapter presents the structural model file and the environmental conditions Before an analysis of the Seafox 2 can be run, however, a number of assumptions and boundary conditions have to be set to limit the number of simulation runs required. These are discussed below.

Waves

The waves at each location described in chapter 4.3 have a wave high, period and direction. This information is split up into blocks on the basis of wave height. Testing reveals that the wave height has a dominant influence on the stress distribution in the legs.. Each block has a wave range of 1 m meter. The first block contains wave of a height between 0-1m, the next block, 1-2m, then 2-3m, etc. The waves periods are the averaged for each wave block. From the scatter plots (chapter 4.3) at each location periods that correspond to the wave heights are determined. The wave heights are averaged, weighted by the number of occurrences and then averaged again for all different locations. Finally, one extra wave block is added to incorporate the dynamic response around the resonance frequency of the structure. This additional wave block of *1,51 m* to *2,06 m* has a mean period of *5,2 s* which is the same as the first mode of vibration of the Seafox 2 (T_n = 5,2 s). This procedure reduces the number of runs from 14x14=196 needed to fully incorporate dynamic effects to a more manageable 14 runs. .

Table 5-1 Wave range with corresponding period

Wave range [m]	**Mean period T_m [s]**
0,00: 1,00	3,9
1,00: 1,51	4,3
1,51: 2,06	5,2
2,06: 3,00	5,9
3,00: 4,00	6,5
4,00: 5,00	7,4
5,00: 6,00	7,6
6,00: 7,00	7,9
7,00: 8,00	8,5
8,00: 9,00	8,8
9,00: 10,00	9,1
10,00: 11,00	9,6
11,00: 12,00	10,1
12<	10,3

As the Seafox 2 has slender legs the modelled wave type (Airy stretched, Airy extrapolated or Stokes 5th) has effect on the force of the structure (chapter 3.1.2). Considering the depth, wave heights and wave lengths encounter by the structure, a stokes 5th wave is chosen.

All waves are assumed to come from the same direction of 225 degrees. This is a very conservative assumption and worst case scenario. The actual waves come from varying directions and spread the load during the lifetime of the rig and the chosen direction of 225 degrees maximizes the stresses on the legs.

Wind

The assumption is made that the wind direction is the same 225 degrees as the wave direction. This is not necessarily always the case but would hold generally over a 30-year life span. This is also the direction where the wind exerts the largest amount of force on the structure, increasing the conservatism of the estimates.

The wind force calculated in section 4.3 is loaded in the model as point loads. The total wind force is then divided by the 48 connection points from hull to the legs in the horizontal plane. A horizontal node load is then set at every hull -leg connection at 225 degree.

The wind load is modelled as a static force. The reasoning behind this is that the period of oscillation for wind gusts (30 to 300s) is considerably higher than the natural periods of Jack-ups (<10s). A static force will not influence the stress range. It is added because due to the non-linearities in the structure it can amplify other forces.

Current

Current invokes stress fluctuations on the structure with a very high period, therefore it is also modelled as static force. A static force will not directly change the stress range in the legs but as the structure is non-linear its inclusion is appropriate as it can amplify other loads.

Table 5-2 Current profile

Height from seabed Z	current factor
5	0,7197
15	0,7946
20	0,842
25	0,8773
30	0,9057
35	0,9296
40	0,9503
45	0,9913
46,2	1

The current profile is given by (P.J. Knight M.J. Howarth D.F. Flatt and S.G. Loch, 1992)

5.2 Member stress results

With all parameters set, the simulation can now be run to determine the stress range. To visualize the stresses, the Von Mises stress for a run with a wave height of 11,5 meters is displayed in Figure 5-1 and Figure 5-2. The highest stresses are found just below the lower guide frame.

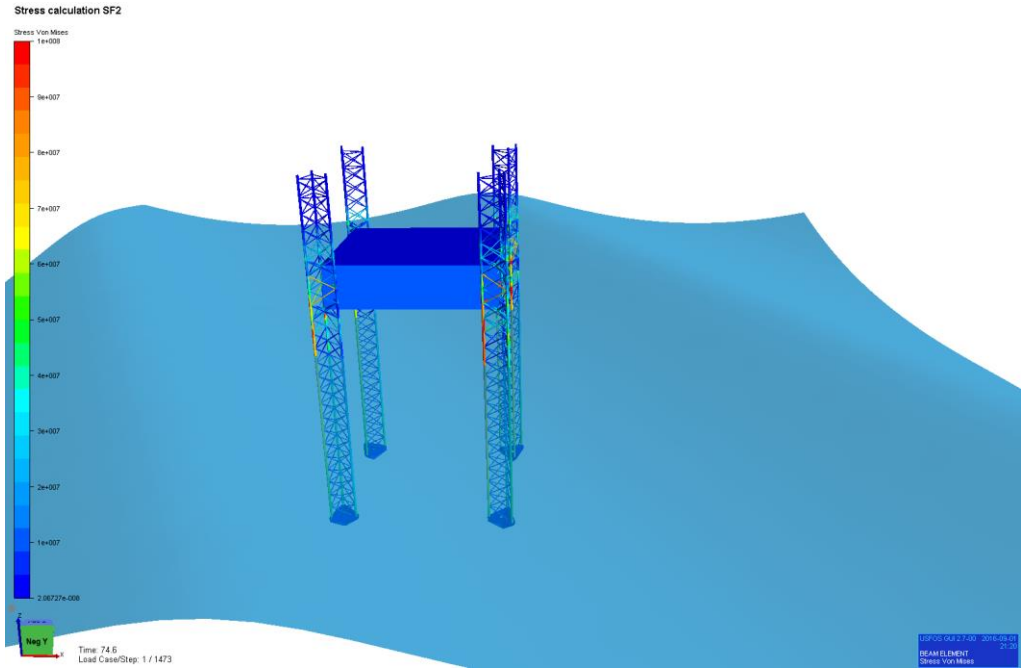

Figure 5-1 Example of the model run at wave height 11,5m

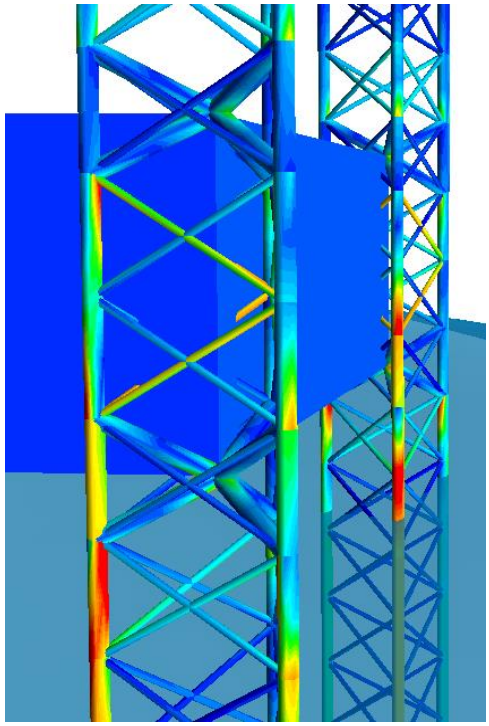

Figure 5-2 Von Mises stress in the legs around the jacking system

The model runs allow for a determination of the joint with the highest stress range. This proved to be the same joint for each of the wave blocks and is located just below the lower guide frame of jack-up leg. This critical joint will be used as proxy to determine the fatigue life of the complete structure. The stress range from axial, out of plane bending and in plane bending in this joint is calculated. Figure 5-3 to Figure 5-5 show examples of the stress range calculation results at a wave height of 4,5m.

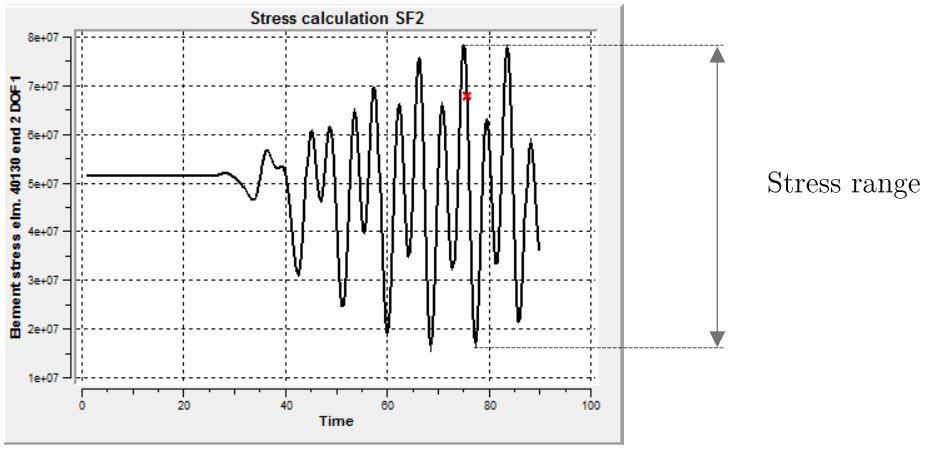

Figure 5-3 Axial (DOF 1) stress over time brace 40130

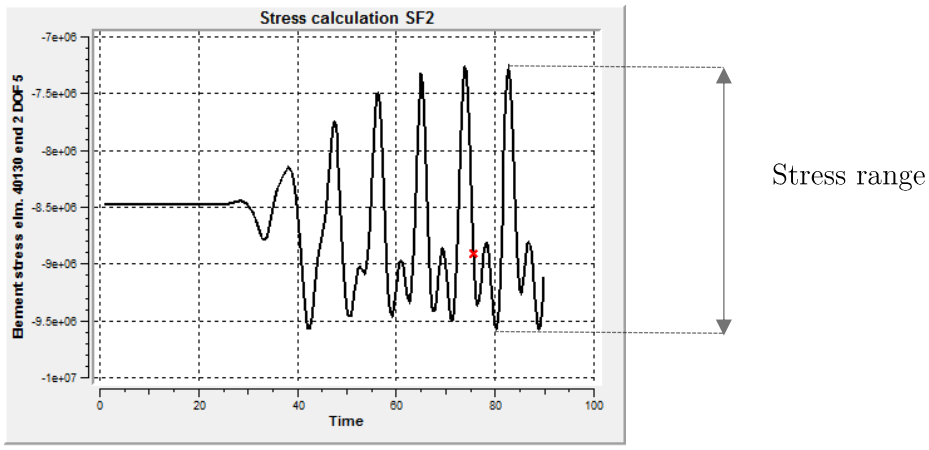

Figure 5-4 Out of plane bending (DOF 5) moment over time

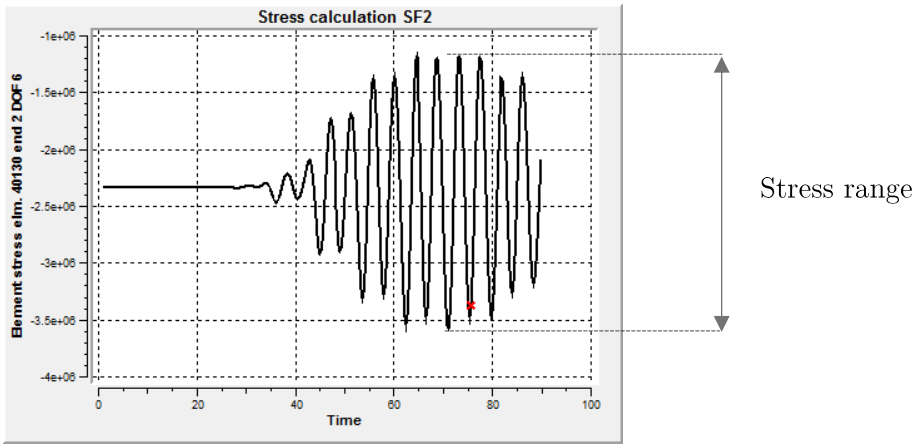

Figure 5-5 In plane bending (DOF 6) moment over time

5.3 Stress concentration factor (SCF)

As discussed in section 2.4, this study uses two methods for calculating the SCF's: the parametric equations of Efthymiou and a finite element model. Efthymiou's parametric equations have proven to give good estimations on simple uni-planar joints but not for more comprehensive multi-planar KK-joints. As noted by DNV-GL "For multi-planar tubular joints for which the multi-planar effects are not negligible, the SCFs may either be determined by a detailed FEM analysis of each joint or by selecting the largest SCF for each brace among the values resulting from considering the joint to be a Y, X and K joint". This study uses both the Efthymioiu's parametric equations and the detailed FEM analysis to determine the SCF's for a single joint. The selected joint is the same critical joint identified in section 5.2.

5.3.1 Efthymiou SCF calculation

Dimensionless geometry parameters (Figure 5-6) serve as input for Efthymiou's parametric equations. The equations give SCF's for both the chord and the bracing for axial load, in plane bending, and out of plane bending. The equations are given in Table 5-4

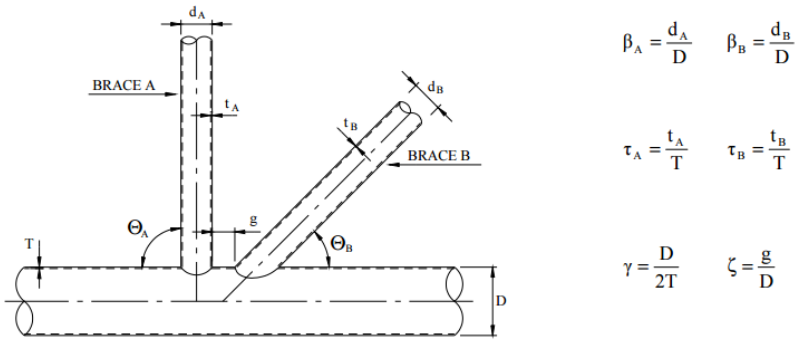

Figure 5-6 K joint geometry

Table 5-3 Dimensionless parameters for joint geometry

Parameter	Value	Valid range	Valid
β	0,4075	$0.2 \leq \beta \leq 1.0$	yes
τ	0,3571429	$0.2 \leq \tau \leq 1.0$	yes
ϒ	4,2857143	$8 \leq \gamma \leq 32$	no
ς	0,1106667	$-0.6\beta / \sin(\theta) \leq \zeta \leq 1.0$	yes

Notable is that Υ does not lie in the validity range of Efhtymiou's equations. The implications of this fact will be tested with the finite element analyses.

Table 5-4 Efthymiou's parametric SCF equations

Axial load	Chord	$\tau^{0.9}\gamma^{0.5}\,(\,0.67-\beta^2+1.16\beta\,)\,sin\theta\,\left(\frac{sin\theta_{max}}{sin\theta_{min}}\right)^{0.30}\,\left(\frac{\beta_{max}}{\beta_{min}}\right)^{0.30}(1.64+0.29\,\beta^{-0.38}\;\;arctan(8\zeta))$	(5-1)
	Brace	$1+(1.97-1.57\beta^{0.25})\tau^{-0.14}\,(sin\theta)^{0.7}\;\;(Eq.\,(5\text{-}1)+(sin(\theta_{max}+\theta_{min}))^{1.8}\;\;(0.131-0.084\,\arctan(14\zeta+4.2\beta))\;C\;\beta^{1.5}\gamma^{0.5}\tau^{-1.22}$	(5-2)
In plane bending	Chord (crown)	$1.45\,\beta\,\tau^{0.85}\,\gamma^{(1-1.05\,\beta)}\,\sin(\theta)^{0.7}$	(5-3)
	Brace (crown)	$1+0.65\beta\tau^{0.4}\,\gamma^{(1.09-0.77\beta)}\,\sin(\theta)^{(0.06\gamma-1.16)}$	(5-4)
Out of plane bending	Chord (saddle)	$\gamma\,\tau\,\beta\,(1.7-1.05\beta^3\,\sin\theta^{0.7}\,(1-0.08(\beta\gamma)^{0.5}\exp(0.8x))+\gamma\,\tau\,\beta\,(1.7-1.05\beta^3\,\sin\theta^{0.7}\;\;(1-0.08(\beta\gamma)^{0.5}\exp(0.8x))\;\;(2.05\beta^{0.5}\exp(-1.3x))$	(5-5)
	Brace (saddle)	$\tau^{-0.54}\gamma^{-0.05}(0.99-0.47\beta+0.08\beta^4)\,\gamma\,\tau\,\beta\,(1.7-1.05\beta^3\,\sin\theta^{0.7}\,(1-0.08(\beta\gamma)^{0.5}\exp(0.8x))+\gamma\,\tau\,\beta\,(1.7-1.05\beta^3\,\sin\theta^{0.7}\;\;(1-0.08(\beta\gamma)^{0.5}\exp(0.8x))\;\;(2.05\beta^{0.5}\exp(-1.3x))$	(5-6)

The resulting stress concentration factors, given in Table 5-5, are rather low due to the geometry of the K-brace. τ which is the ratio between the wall thicknesses of the brace and the chord is low which will lead to a decrease in SCF. Υ which gives the ratio between chord diameter and wall thickness is so low it lies out of the validity rage. This will also lead to a decrease in SCF.

It appears that the structural engineers have actively tried to combat high hot spot stresses in the geometric design of the Jack-up legs.

Table 5-5 Resulting SCF's

Axial	SCF_C	0,7806147
	SCF_B	1,4180725
In plane bending	SCF_{CC}	0,4364399
	SCF_{BC}	2,0081683
Out of plane bending	SCF_{CS}	0,421856
	SCF_{BS}	0,5476309

5.3.2 FEM SCF calculation

RFEM software is used for the finite element analyses of the joint. RFEM is a FEM software package used at Seafox. Joint modelling and mesh sizing can be done with a higher level of detail than in USFOS. A single joint is modelled using a solid tube element, one chord and four braces.

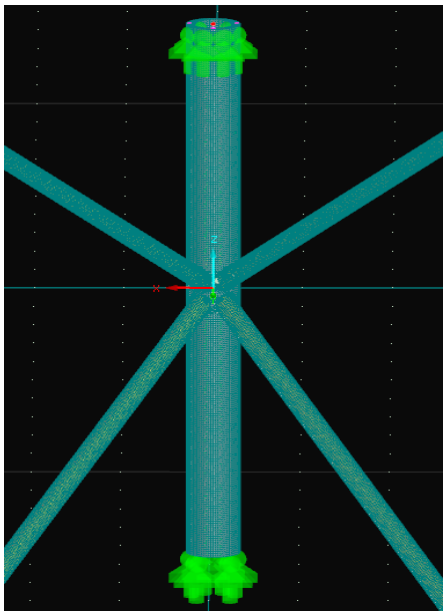

Figure 5-7 Modelled joint in RFEM

After the joint is modelled a mesh is generated. Smaller mesh size will return a more accurate solution but will increase computing power. DNV-GL recommends at least 4 mesh elements in thickness direction. The axial-, in plane bending- and out of plane bending load simulations are run separately giving the SCF results shown in

Table 5-6 SCf's from FE model.

The results from the FE model do not differ from the Efthymiou equations by more than 10%, except the out of plane bending moment SCF, where there is a difference of 32%. It is plausible the latter difference is caused by the carry-over effect, caused by braces effecting each other in multiple planes (difference K-joint and KK-joint). The out-of-plane bending SCF is low and these stresses are not significant. Thus, this difference is deemed acceptable and is not researched further. The calculations of the hot spot stress ranges uses the SCF's results from the FE model.

Table 5-6 SCf's from FE model

Axial	SCF_C	0,62
	SCF_B	1,66
In plane bending	SCF_{CC}	0,53
	SCF_{BC}	2,32
Out of plane bending	SCF_{CS}	0,62
	SCF_{BS}	0.82

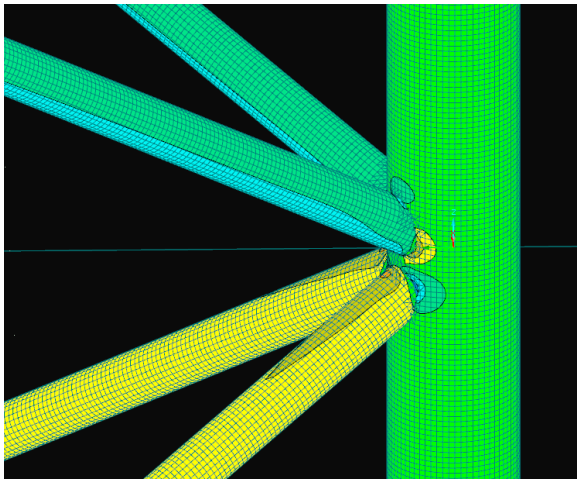

Figure 5-8 Axial loads

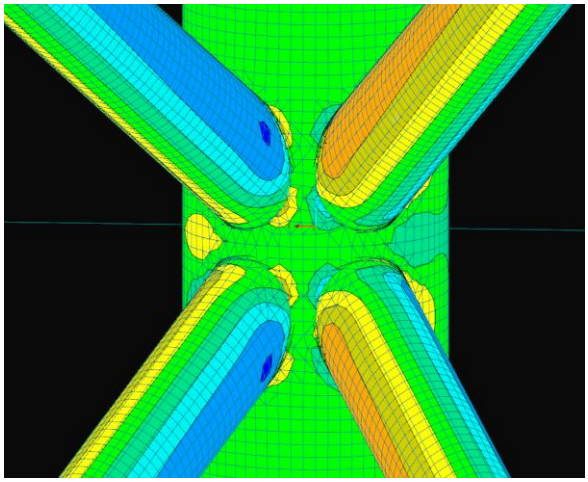

Figure 5-9 Out of plane bending loads

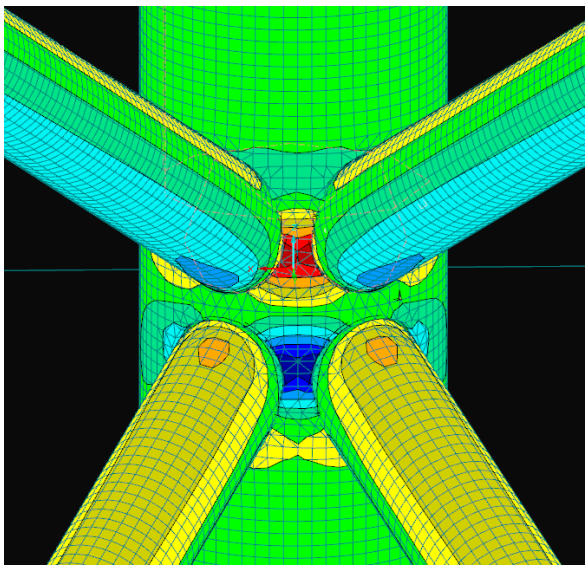

Figure 5-10 In plane bending loads

5.4 Results

5.4.1 Fatigue life calculation

Stress, number of cycles and SCF's are known. The fatigue life of the critical joint can now be calculated with Eq. 6.3 in which N is the number of cycles until failure and $\Delta\sigma$ is the stress range from the USFOS model . The other parameters are given in Table 5-7.

Eq. 5.3

$$\log N = \log \bar{a} - m \log\left(\Delta\sigma \left(\frac{t}{t_{ref}}\right)^{k}\right)$$

Table 5-7 S-N curve parameters from (DNVGL-RP-C203, 2016)

Parameter	Meaning	Brace	Chord
log a ¯	Intercept of log N axis	15,606	15,606
t	Thickness through which a crack will most likely grow	32	60
tref	Reference thickness = 32mm for tubular joints	32	32
k	thickness exponent on fatigue strength is 0,1 for tubular butt welds	0,1	0,1
m	Negative inverse slope of the S - N curve	5	5

In Table 5-8 the fatigue damage is given as fraction of the damage till failure. Where a fatigue damage of 1 would lead to failure. The fatigue damage is given per wave block, from Palmgren-Miner we know these damage fractions can be summated to give the total damage in the joint.

Table 5-8 Results fatigue calculation for critical joint

Wave block	Number of cycles	Hot spot stress	Log N	N	Damage
0,00: 1,00	9,62E+07	8,12E+06	11,06	1,14E+11	0,00084109
1,00: 1,51	2,80E+07	1,51E+07	9,71	5,11E+09	0,00547644
1,51: 2,06	2,24E+07	1,82E+07	9,30	2,00E+09	0,01116252
2,06: 3,00	6,90E+06	2,25E+07	8,85	7,00E+08	0,00985387
3,00: 4,00	1,74E+06	3,14E+07	8,12	1,33E+08	0,01306902
4,00: 5,00	4,95E+05	4,16E+07	7,51	3,24E+07	0,01527306
5,00: 6,00	1,50E+05	5,16E+07	7,04	1,10E+07	0,01357651
6,00: 7,00	4,70E+04	6,11E+07	6,68	4,74E+06	0,00991131
7,00: 8,00	1,49E+04	7,35E+07	6,27	1,88E+06	0,00792028
8,00: 9,00	4,75E+03	8,65E+07	5,92	8,34E+05	0,00569836
9,00: 10,00	1,45E+03	1,15E+08	5,29	1,97E+05	0,00734432
10,00: 11,00	4,47E+02	1,43E+08	4,83	6,75E+04	0,00662425
11,00: 12,00	1,89E+02	1,65E+08	4,52	3,30E+04	0,00573420
12<	1,64E+01	2,15E+08	3,94	8,79E+03	0,00187090
			Total damage		0,114356

The Seafox 2 has been in service for, 30 years. Therefore the fatigue life of the critical joint is $\frac{30}{Total\ damage}$ = 262,3 years. As the stress range is highest in the critical joint, is deemed governing for the integrity of the whole structure. The critical joint is used as proxy to determine the fatigue life of the Seafox 2. Therefore the fatigue life of the Seafox 2 is 262,3 years.

Calculation of the fatigue life is associated with a lot of uncertainty. Due to the non-linearity of the S-N curve minor changes in stress range cause large fluctuations in fatigue life. Therefore high fatigue design factors are set by classification societies. The fatigue design factors depend on accessibility for inspection and the availability of one or more alternative load paths (redundancy) after failure. ISO 19905 states: recognized classification society approved Jack-ups with braced legs are do not have single members or member connections that, when damaged, can cause a failure with major consequence. Therefore the design safety factor for legs structures in the splash zone is 3. Applying this design factor will lead to a fatigue life reduction with a factor 3. The Seafox 2 can still remain operational when applying

The results for the Seafox 2 are promising and according to this analyses the Seafox 2 can remain operational. Due to the conservativeness of this analyses this conclusion only works one way. If results of this study had shown a fatigue life less than 30 years this would not mean the Seafox 2 could not operate anymore. In this case a less conservative analysis could be conducted.

Table 5-9 Fatigue damage design factor for redundant structures. (ISO 19905)

Description (assumes there is structural redundancy for every member and member connection)			**Fatigue damage design factor,** $f_{FD,s}$
Can inspect and repair	Hull structure	Primary hull structure	1
		Leg-to-hull interface structure with access for inspection and repair	2
	Leg structure in air	Leg chords, brace to chord joints, brace joints	2
Can inspect but not repair	Leg structure in splash zone	Leg chords, brace to chord joints, brace joints	3
	Leg structure under water	Leg chords, brace to chord joints, brace joints, leg to spudcan connection	3
	Spudcan	Structure with access for inspection and repair	3
Cannot inspect or repair	Hull structure	Leg-to-hull interface structure without access for inspection and repair	5
	Leg structure under sea floor	Leg chords, brace to chord joints, brace joints, leg to spudcan connection	5
	Spudcan	Structure without access for inspection and repair	5

5.4.2 Comparison of fatigue analyses

In 1983 Marine Structure Consultants (MSC) bv conducted a fatigue analyses for the Seafox 2. It was only conducted for the Morecambe Bay gas field in the Irish Sea. The analyses starts by defining a long term sea state distribution and choosing five significant wave heights with the appropriate periods and probability of occurrence. MSC use a computer program (DYNSEP) to solve the unit's equation of motion in the time domain and account for non-linear effects due to current and drag.

The analyses shares some similarities with the analysis in this thesis: the analysis is a dynamic one conducted in the time domain. The analyses also uses wave blocks to describe environmental conditions. However a stochastic approach is used to define wave heights opposed to a deterministic approach used in this thesis. To quantify the accuracy of the analysis conducted in 1983 with a stochastic approach, one must acknowledge there are a lot unknowns and differences in the analyses. The report from 1983 does not comment on:

- The fixity of the leg – ground interface.
- The stiffness of the hull – leg interaction.
- The stiffness of the hull.
- The used SCF's.

Therefore the environmental input parameters are compared and fatigue life are compared in the following paragraphs.

Environmental input data

The analyses uses five arbitrarily chosen wave blocks and gives the probability of not exceeding the significant wave in this block. The actual environmental data encountered by the Seafox 2 is split into the same arbitrarily chosen wave blocks as in the 1983 study. The wave blocks with wave period and probability of not exceeding, used in 1983 fatigue analysis and calculated probability of not exceeding are given in Table 5-10.

Table 5-10 Comparison of probability of not exceeding a wave height

Block No.	HS m	TZ sec	P %	P_{actual} %
1	1.5	3.92	93.58	88,65
2	3.0	5.54	5.86	9,13
3	4.5	6.79	0.51	1,95
4	6.0	7.84	0.04	0,19
5	7.5	8.76	0.01	0,07

Striking difference is the higher probability of encountering higher waves in the actual environmental data. The wave data used in 1983 only describes the environmental conditions in the Irish Sea which could explain the difference.

Design data

The design data used in 1983 is comparable with the parameters used in this thesis. The analyses conducted in 1983 uses the same very conservative angle of attack for all waves and the other parameters are comparable. The design data is found in Table 5-11.

Table 5-11 Design data from study 1983 and this thesis

	1983	2016	
- waterdepth	40 m	42.2	[m]
- current velocity	0.6 m/sec.	0.8	[m/s]
- platform weight	5400 tf (central)	5815000	[kg]
- penetration	3 m	2.7	[m]
- angle of waves	225.0^{0}	225	°

If the unknowns from the 1983 analyses mentioned in the beginning of this section are not taken into account and the design data are considered equal in the two fatigue analyses, the only difference remaining is the wave data. The resulting difference in fatigue life can then be attributed to the different wave data. The results for fatigue life in the 1983 analyses are given in Figure 5-11 Results of the fatigue analyses conducted in 1983 The analyses from 1983 gives a fatigue life of 600 year in the brace – chord connection. The fatigue life of the brace – chord connection calculated in this thesis is 262,2 years. This difference can then be ascribed to the different conditions in the Irish Sea and other locations in where the Seafox 2 has operated. Or the difference comes from the two different ways for determining environmental conditions. Either way the hindcasting method can attribute to a more comprehensive way for describing environmental loading for multiple locations. This method especially ads value when a Jack-up has operated in different locations.

The main results of the fatigue calculation are:

a. Brace to chord connection	=	600 year
b. Chord buts weld	>	1000 year
c. Hull	>	1000 year
d. Jacking system	>	1000 year

Figure 5-11 Results of the fatigue analyses conducted in 1983

6 Influence of corrosion

As mentioned in the introduction, this thesis started as an investigation of the influence of fatigue damage on a Jack-ups in different environmental locations. Ultrasonic thickness measurement (UTM) examination on the Seafox Burj made as this study was underway showed significant steel diminution. For commercial reasons Seafox wanted to know if the legs needed to be replaced unconditionally or if the Burj could still operate in lower water depths without leg replacement. This question was added to the scope of the thesis and is addressed in the following chapters.

6.1 The Burj

The Burj is a three legged, non-selfpropelled, self-elevating accommodation unit (jack-up). It was designed and built as a Jack-up mobile drilling rig in by LeTourneau and completed in 1972. It was acquired by Seafox in 2011 and refitted for a second life as accommodation unit. Major upgrades were made, drill equipment was removed, and a crane was added. No major maintenance was performed on the rig legs all this time.

The Burj came into dock in 2015 for a major overhaul on legs, tanks and structural components. Determining the influence of diminution of the operational readiness of the Burj is of significant commercial interest to Seafox as it may indicate which work scopes are acceptable without major retrofitting of the legs.. The Burj is checked on survival conditions and ultimate limit state (ULS).

Figure 6-1 Seafox Burj

6.2 Basics of corrosion

Corrosion is the deterioration of a metal that results from its electrochemical or chemical reaction to the surrounding environment.

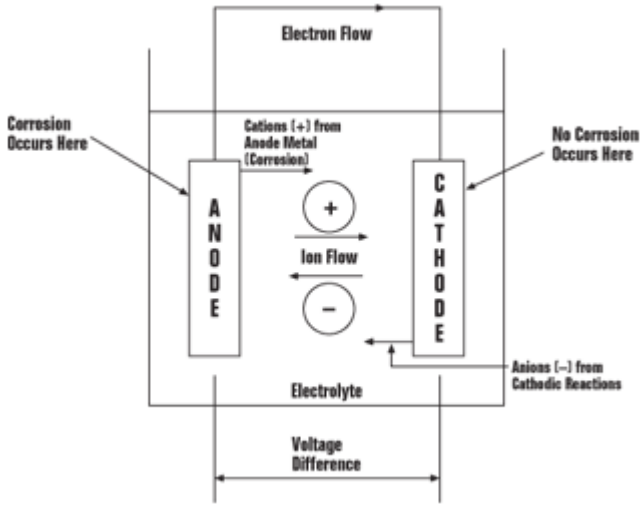

6.2.1 Local corrosion

Localized corrosion refers to the deterioration of specific areas of a surface. This effect is primarily caused by the influence of environmental conditions on the exposed material. Localized corrosion can be categorized as pitting, fretting, cavitation, crevice, and filiform. (Singh, 2014) Pitting is described as a hole or cavity that occurs in a localized corrosive area of a material. Perhaps the most common way pitting is initiated is by the electrical circuits that are created through the impurities of metals. Any breaks in the protective coating or passive film of the material are additional causal factors for corrosion.

6.2.2 General corrosion

General corrosion is the most simplistic form of corrosion and . It refers to the rate at which a metal uniformly diminishes, creating byproducts commonly referred to as rust.

General corrosion is the main form of corrosion on the Burj legs. Although the UTM reports shows some pitting, it is highly spread out and not located at high stress areas e.g. the joints. This thesis focuses on only the steel diminution from general corrosion and the minor pitting is not taken into account.

6.3 Modelling the Burj

Like the Seafox 2, The Burj is modelled in USFOS to determine stresses in the legs. Nodes are created by assigning x-y-z coordinates. Beams, plates and shell-elements are generated between the nodes and given material and geometry data. Furthermore, spring elements, structure to ground connections (rotational springs), gravity, flooded and non-flooded sections, and loads etc. are added to make a complete model. The whole model is extensive and comprises of over 2500 nodes and almost 4500 beam elements. In the following paragraphs the essential and defining components are discussed. The whole input file is found in appendix E.

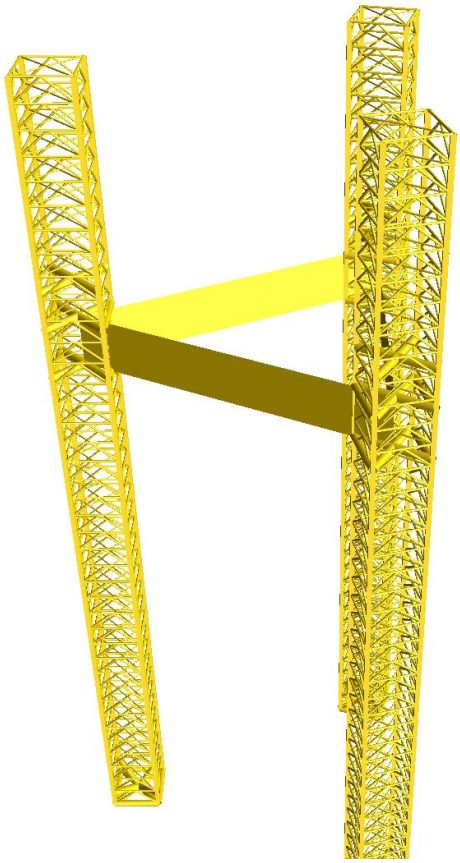

Figure 6-2 Structural model of the Burj

6.3.1 Legs and leg to ground interface

The Burj truss legs consist of four chords interconnected by horizontal and diagonal k-bracing. All the braces are tubulars with different diameters, thicknesses and yield strengths described in section 6.3.2.

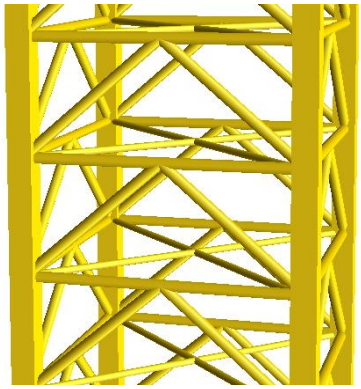

Figure 6-3 Leg section of the Burj

Table 7-6-1 Bracing properties

Cross-Section	Moments of inertia [cm^4]			Cross-Sectional Areas [cm^2]		
Description [mm]	Torsion J	Bending I_y	Bending I_z	Axial A	Shear A_y	Shear A_z
RO 323.9x19.05 | ANSI B 36.10M	42478,40	21322,60	21322,60	182,89	90,91	90,91
RO 219.1x8.18 | ANSI B 36.19M	6028,32	3018,69	3018,69	54,20	26,90	26,90
TR 711/50/25/770/120/250	271075,14	694555,78	281517,72	934,34	343,28	266,31
RO 323.9x25.4 | ASTM A 53	53400,00	26700,00	26700,00	238,00	118,66	118,66
RO 323.9x12.7 | ASTM A 53	30100,00	15100,00	15100,00	124,00	61,62	61,62
Pipe 500/200	612610,57	306305,28	306305,28	1884,96	1235,48	1235,48

6.3.2 Leg chords

The chords of the Burj legs are a non-tubular LeTourneau design. They consists of welded plates with the rack on the outside face. This chord geometry can be modelled in USFOS by using the GENBEAM command, which lets the user define a beam by defining area, moment of inertia in y- z axis and torsional, plastic sectional modulus about y- z axis and torsional and shear area. The hydrodynamic properties of the leg chords are set manually.

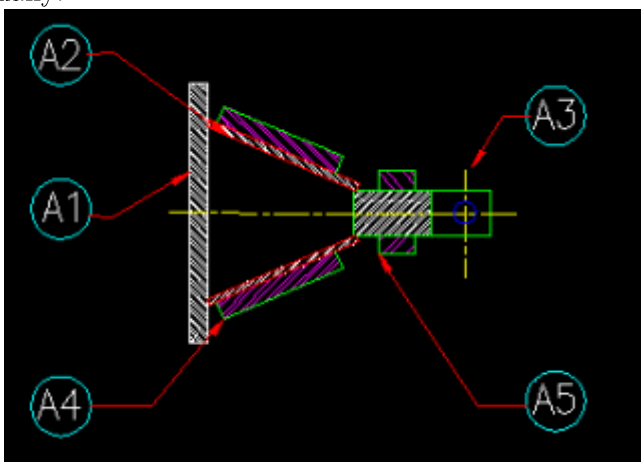

Figure 6-4 Cross section chord of Burj leg

Moment of inertia, yield strength and area calculation of the chords

Modelling the chords requires determination of the moment of inertia and cross sectional area. Old construction drawings were recreated in AutoCad and the moment of inertia from the centreline indicated in yellow, Figure 6-4 was calculated.. The chords of the Burj are comprised of different steel types as shown in Table 6-2. The yield stress of the chord is calculated by considering the effective area of the different chord components.

Table 6-2 Cross section details as seen in Figure 6-4

Selection nr.	Item	Area [m]	Moment of enertia [m4]	Yield strength [ksi]
A1	Back plate	0,0365	0,0235	70
A2	Side plate	0,0168	0,0110	70
A3	Rack	0,0402	0,0110	85
A4	Flat bar	0,0365	0,0315	85
A5	Flat bar	0,0094	0,0238	70
Total		0,1393	0,100859	78

Given these attributes the leg chords are modelled as a hollow box section with the dimensions given in Table 6-3

Table 6-3 Modelled chord dimensions

Box element		
H	0,71	[m]
W	0,71	[m]
$\mathbf{t_{side}}$	0,0530	[m]
$\mathbf{t_{bottom}}$	0,0530	[m]
$\mathbf{t_{top}}$	0,0530	[m]
A	0,1393	[m^2]
$\mathbf{I_y}$	0,0100855	[m^4]
$\mathbf{f_y}$	537,8	[N/mm^2]

Hydrodynamic properties

The hydrodynamic properties are also manually set according to the SNAME 5-5A guidelines where the drag coefficient is related to the projected diameter. The drag coefficient C_D for the different angles of attack are given in Table 7-6-4.

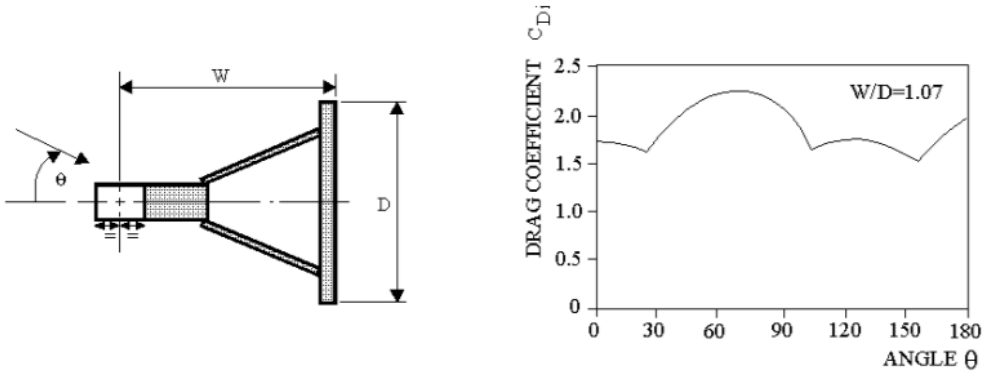

Figure 7-6-5 C_d with corresponding angle of attack

Table 7-6-4 C_d for different angles of attack

Angle of attack [degrees]	C_d [-]
0	1,70
45	2.05
90	1.95
135	1.70
180	2.0

The inertia coefficient $C_{Mi} = 2.0$ (as for a flat plate), related to the equivalent volume of $\pi D_i^2/4$ per unit length of member, is applied for all headings (SNAME 5-5A).

Spudcans

The spudcans are modelled as, rigid beam elements. This gives an accurate transfer of the seabed reaction into the leg chords and bracing. (NEN-EN-ISO, 2012).

6.3.3 hull - leg interface

The Burj has a rack and pinion jacking system. The jacking is done by “driving” the motorized pinions up and down the chord. The racks are positioned on the outside face of the chords, where they interlock with unopposed jacking pinions.

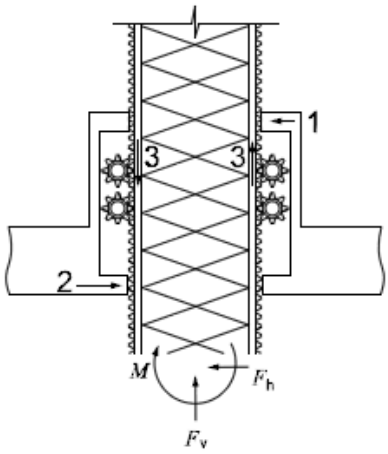

Figure 7-6-6 Rack and pinion jacking system with unopposed pinions

In many ways the hull - leg interface of the Burj is modeled the same as the Seafox 2. With rigid beams connected to the chords with 6 DOF springs. Major exception is the rack and pinion jacking system. Unlike the floating pin and hole system in the Seafox 2 the rack and pinion system does absorb loads in the horizontal plane.

The stiffness of the rack and pinion system were provided by the manufacturer, as follows:

- Vertical stiffness = 6,224 10^9 N/m (per chord)
- Lateral stiffness 1,392 10^9 N/m (per chord)
- Rotational stiffness = 7,629 10^{11} $Nm/radian$ (per chord)

A local coordinate system is created for the springs. This is to align the local x direction with the x direction of the rigid beams. The lateral stiffness is collinear to the rigid beam.

Table 6-5 Modelled spring stiffness of the jacking system

k_x	1,392 10^9
k_y	1
k_z	6,224 10^9
k_{rx}	7,629 10^{11}
k_{ry}	1
k_{rz}	1

As with the Seafox 2 the guide frames are assumed to be rigid and are free in the vertical plane.

6.3.4 Legs to ground interface

Each of the three spudcans are connected to the ground by means of a (6 DOF) spring. For calculation of the ultimate limit state the most conservative supports are chosen. As with the Seafox 2 these are pinned supports with zero fixity. See section 4.2.4 for a more detailed description.

6.3.5 Alternatives considerations

The Burj is modelled in the same manner as the Seafox 2 and so the same considerations hold as discussed in section 4.2.5. However, the Burj was subjected to a previous dynamic analyses to assess survival conditions. This work yields benchmarks against which the study results can be benchmarked, with regards to dynamic response and the unity check for structural strength.

7 Stress increase due to diminution

In this chapter the influence of diminution on the tolerable survival conditions is investigated in shallow, intermediate, and deep water. The model is run in a number of diminution stages to plot the stress increase in the members as a result of diminution. Unity checks are done for the critical members for each diminution stage. The study uses finite element method analyses on the constructed model in the time domain to check excessive yield and buckling of structural members.. The FEM analyses is conducted in the time domain to account for the non-linearities described in section 3.

7.1 Environmental conditions

For commercial reasons the chosen shallow and intermediate water depth locations are places where Seafox might be able to secure a contract. They are: the North field in the UEA with a shallow water depth and the Al Shaheen field in the Persian gulf which has intermediate water depths. The analysis includes the deep water Bayu Udan field in East Timor, where the Burj worked before it came off contract. The deep water scenario functions as a benchmark for the model as a previous ULS check was performed by a marine consulting firm.

The reference wave height for the elevated (survival) condition for a specific location is the 100 year wave, H_{100}, defined as the maximum wave with a return period equal to 100 years. The 100 year storm conditions at each location are given in Table 7-1 to Table 7-2.

Table 7-1 Survival conditions Bayu Udan

Bayu Undan (East Timor)		
Water Depth	82,3	[m]
Wave height	12,6	[m]
Wave period	9,96	[s]
Wind velocity	31,9	[m/s]
Current velocity	0	[m/s]
Air gap	10,7	[m]
Penetration	7,6	[m]

Table 7-2 Survival conditions North Field

North Field (UEA)

Water Depth	43,9	[m]
Wave height	5,5	[m]
Wave period	9,8	[s]
Wind velocity	30,4	[m/s]
Current velocity	0,9	[m/s]
Air gap	10	[m]
Penetration	5,5	[m]

7.2 Steel diminution of the Burj

Using the actual ultrasonic thickness measurements (UTM) conducted during the maintenance period proved too onerous for this study. The steel thickness was checked on at least 12 locations on every brace and even more on the chords, resulting in almost 4500 elements that would have to be input manually. Therefore, all elements were assumed to have the same diminution. The diminution is expressed as a percentage of material lost, relative to the as built steel thickness, where 0% diminution is the as built thickness. The model is then run for a set of diminution values ranging from 0% to 30%.The diminution is increased with steps of 5 percentage points and the model is run for each diminution step. This way the stress increase due to diminution can be plotted and for each diminution step the structural integrity can be checked.

7.3 Strength check results

The Von Mises stress is displayed in Figure 7-1. It shows that, like the Seafox 2, the highest stresses on the Burj are found just below the lower guide frame.

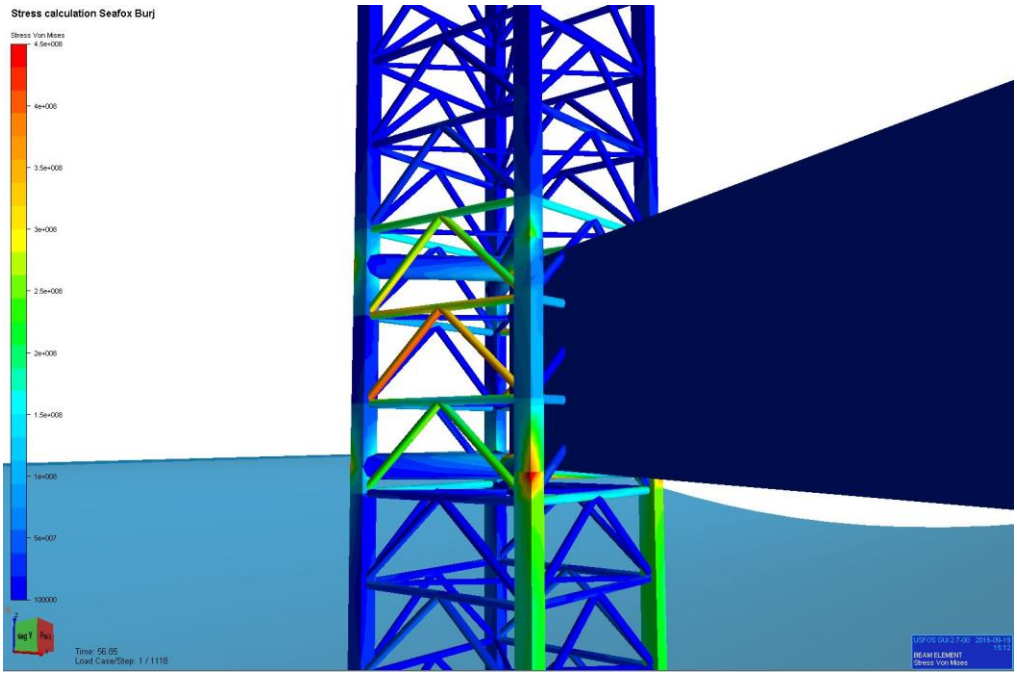

Figure 7-1 Von Mises stress for 100 year storm Al Shaheen field

Yielding and buckling can both be checked by running a yield or buckling analysis directly in USFOS. However there is no function in USFOS to retrieve exact values of the exact yielding and buckling as a percentage of the yield strength. The software merely produces a colour range. Therefore, maximum stresses are retrieved for each percentage of diminution and a manual unity check is performed. Table 7-3 gives the results for the North field. The results for Al Shaheen and Bayu Udan are found in Appendix B. The stresses are calculated separately in the chords, horizontal bracing and diagonal bracing. For each a unity check is performed.

Table 7-3 Member stress for survival conditions in the North Field

	North Field					
0%		yield strength [ksi]	yield strength	stress	Stress increase factor	U.C.
	Chord	78	537,8	173	1	0,32
	bracing diagonal	85	586,1	134	1	0,23
	bracing horizontal	85	586,1	136	1	0,23
5%		yield strength [ksi]	yield strength	stress		U.C.
	Chord	78	537,8	180	1,040462	0,33
	bracing diagonal	85	586,1	136	1,014925	0,23
	bracing horizontal	85	586,1	138	1,014706	0,24
10%			yield strength	stress		U.C.
	Chord	78	537,8	191	1,104046	0,36
	bracing diagonal	85	586,1	143	1,067164	0,24
	bracing horizontal	85	586,1	147	1,080882	0,25
15%		yield strength [ksi]	yield strength	stress		U.C.
	Chord	78	537,8	204	1,179191	0,38
	bracing diagonal	85	586,1	152	1,134328	0,26
	bracing horizontal	85	586,1	150	1,102941	0,26
20%		yield strength [ksi]	yield strength	stress		U.C.
	Chord	78	537,8	218	1,260116	0,41
	bracing diagonal	85	586,1	161	1,201493	0,27
	bracing horizontal	85	586,1	158	1,161765	0,27
25%		yield strength [ksi]	yield strength	stress		U.C.
	Chord	78	537,8	238	1,375723	0,44
	bracing diagonal	85	586,1	177	1,320896	0,30
	bracing horizontal	85	586,1	176	1,294118	0,30
30%		yield strength [ksi]	yield strength	stress		U.C.
	Chord	78	537,8	253	1,462428	0,47
	bracing diagonal	85	586,1	185	1,380597	0,32
	bracing horizontal	85	586,1	184	1,352941	0,31
...	...	...	....	....	....	...

The results for the member unity checks for the North Field, Al Shaheen field and Bayu Udan are plotted in Figure 7-2 to Figure 7-4. These graphs show a unity check plotted against each diminution step. The unity check is conducted for the critical joint for each location. This critical joint is located just beneath the lower guide frame. The analysis supports the following conclusions:

- The Burj will not structurally fail due to yielding or buckling in the North field. At 50% diminution the Burj is still able to operate in these water depths.
- For the Al Shaheen field yielding in the chords gets critical over 30% diminution. As in the North field, higher stresses are recorded in the chords. However at this point a detailed ULS analyses is recommended.
- At the Bayu Udan field, plastic deformations in the chords occur at around 7% diminution. For the diagonal- and horizontal bracing plastic deformations occur at 17% and 18% diminution respectively. Furthermore the chords buckle at 22% diminution.

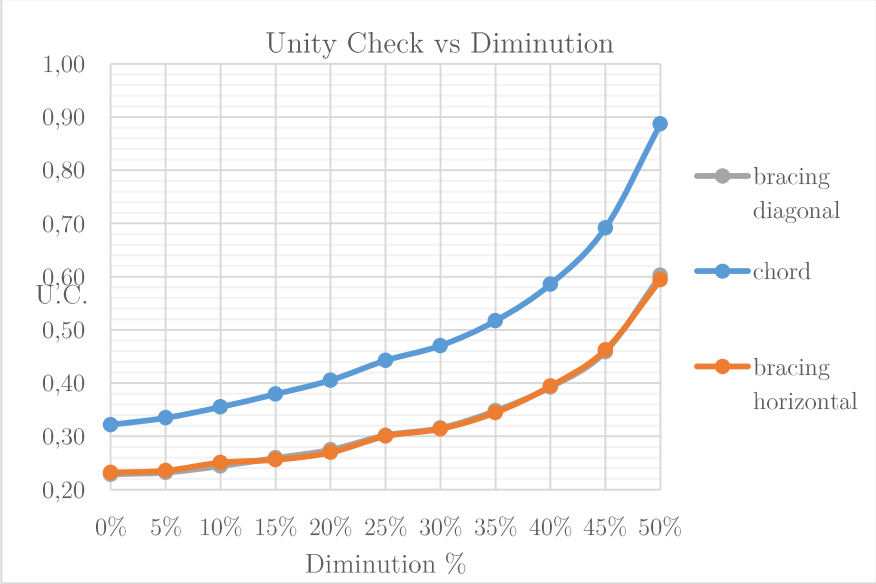

Figure 7-2 North field

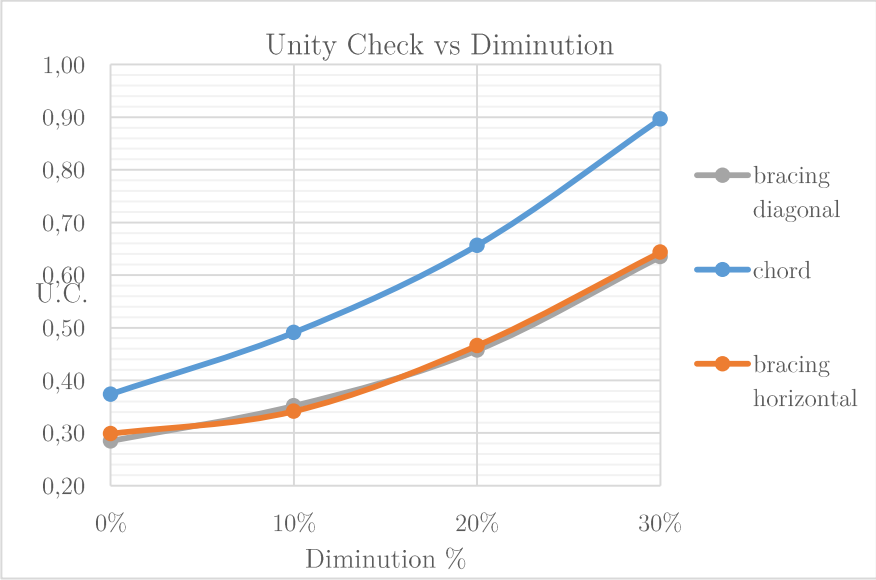

Figure 7-3 Al Shaheen field

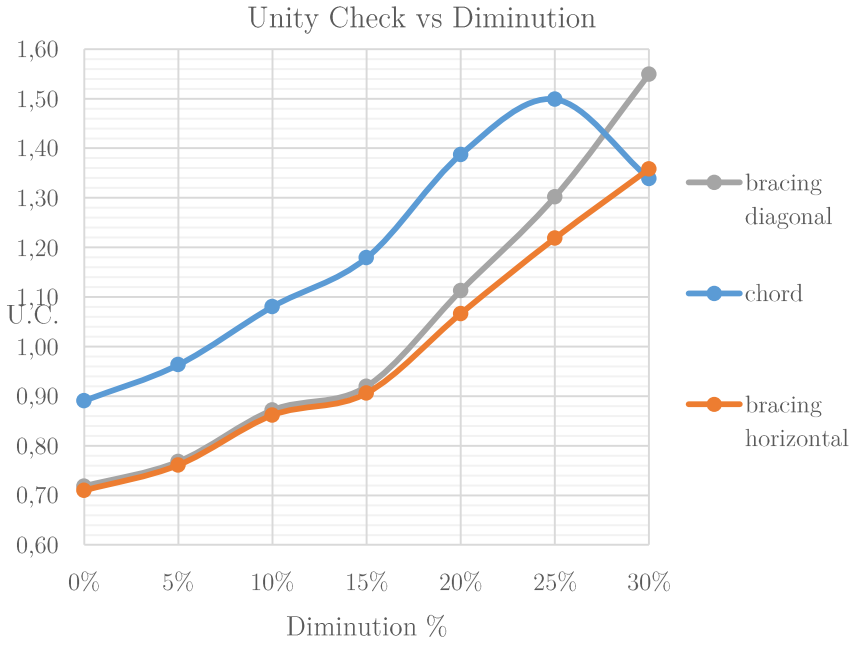

Figure 7-4 Bayu Udan

7.4 Conclusion

Actual steel diminution of the Burj legs varies from 5% to 25% in the most corroded parts. The modelling of diminution between 0% and 30% supports the conclustion that the Burj cannot operate in the deepwater Baju Udan field without drastic maintenance on the legs. It can, however, safely operate in the North field with its shallower water depths.

For Al Shaheen, it might still be possible for the Burj to operate in at these water depths, however the modelling results support the recommendation to do a detailed structural analyses.

8 Effect of diminution on the fatigue life of the Seafox 2

Corrosion can greatly shorten the fatigue life of a structure. Both crack nucleation and crack propagation are influenced by a corrosive environment. A number of studies have been done on crack growth rate on a microscopic level (e.g. Paris and Erdogan (1963)). In practice corrosion fatigue is captured in the S-N curve. Section 2.3.2 discusses the S-N curve for tubulars in air and sea water, - with and without cathodic protection. The S-N curve lowers as less cycles are necessary till failure. The fatigue calculations of the Seafox 2 uses the S-N curve for tubular in sea water with cathodic protection, thus, capturing the effect of corrosion in the fatigue life calculations. However, corrosion and steel diminution have two different effects. The latter is not captured in in the S-N curve. Diminution also have effect on the operational life of the Seafox 2 and is not captured in the fatigue calculations.

Steel diminution of the individual members of the Seafox 2 is not known and Figure 8-1 Stress increase due to is added to this thesis to illustrate the effect of diminution on fatigue life. The steel diminution of the Seafox 2 legs is increased with steps of 5%. For each step the stress range is calculated in the critical joint using the same USFOS analysis as in section 5. The SCF's are also unchanged. The resulting stress range increase in the member caused by steel diminution is plotted in Figure 8-1 Stress increase due to diminution. The stress increase factor is the stress with diminution divided by the stress with zero diminution.

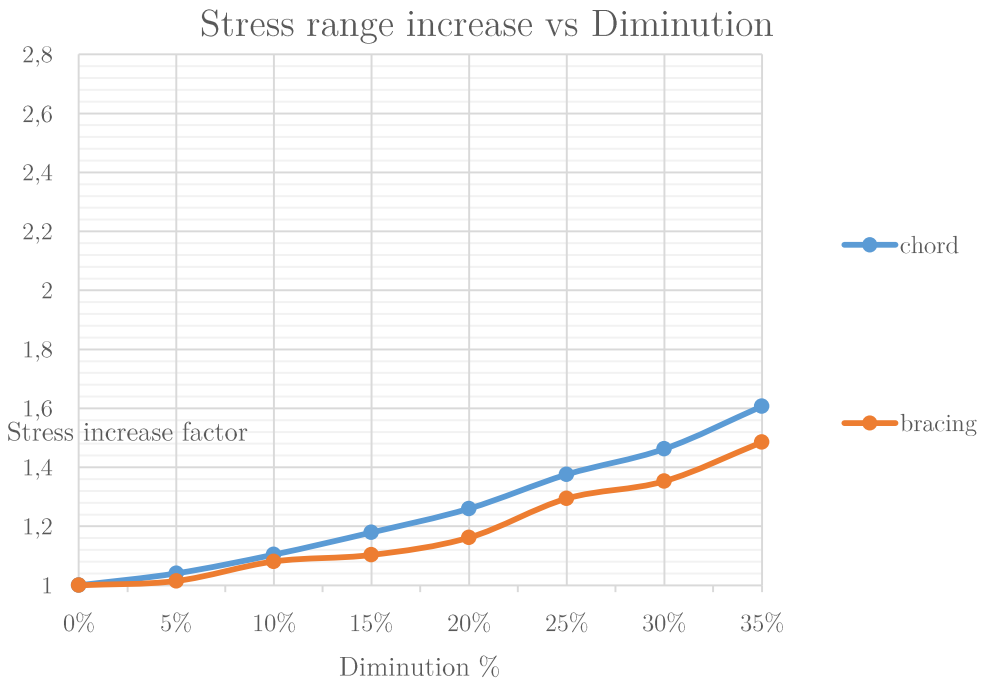

Figure 8-1 Stress increase due to diminution

For example, a rather large diminution of 15% Seafox 2 legs would lead to a stress range increase with a factor 1,2. A stress range increase with a factor 1,2 would lead to a large non-linear decrease in fatigue life.

Further research is needed into the relation between steel diminution and fatigue life

9 Conclusion

The structural characteristics of a Jack-up include various non-linearities justifying a time domain finite element analysis of metal fatigue in the legs (for a frequency domain analyses linearization's are required). These non-linearities include: non-linear structural stiffness, phase differences in loading on the individual legs and non-linear hydrodynamic drag.

There are a number of consideration to take into account when building a load model for a dynamic analysis of a Jack-up. The leg-hull connection has considerable impact on the dynamic response of the Jack-up and therefore on member stresses. When lateral and rotational stiffness's are not supplied by the manufacturer, they can be calculated by taking the pin- and shock pad stiffness into account in a pin and hole jacking system. The stiffness's of the ground connection (fixity) also has considerable impact on the response of a Jack-up. The leg fixity also influences the dynamics of a jack-up. Fixed supports will decrease the natural period of the Jack-up. A lower natural period will lead to resonance at lower wave heights. However, the non-linear increase in member stress associated with resonance at higher wave heights is considered to have a larger effect on fatigue life than the increase in the number of stress cycles at a lower resonance frequency. Therefore the choice of pinned supports is considered conservative. The exact effect of fixity on dynamic behaviour needs more research.

The determination of the stress ranges requires simplifications to reduce the amount of input parameters. These are discussed, noting that caution was taken not to lose significant accuracy. Wave height is found to be the dominant parameter causing member stresses. Waves are therefore categorized in a subset of wave height blocks. To ensure the influence of dynamic response is not lost, an extra wave height block is added around the resonance frequency. The slender legs of a Jack-up mean they are drag dominated and as such caution should be taken when selecting a wave theory. Differences in wave loading for each wave theory are substantial for drag dominated structures. For the water depths and wavelengths relevant for this thesis, the Stokes 5^{th} proved to be the right fit. Wind- and current forces have long periods and can therefore be modelled as static processes.

The member stress ranges are established by running a time domain finite element analyses in USFOS. A stress concentration factor (SCF) is used to determine hot spot stress ranges in Jack-up legs. The study uses two methods for calculating the SCF's: parametric equations of Efthymiou and finite element analyses. The results from the two

methods do not differ more than 10%, providing confidence in the model results. Finally, the fatigue life of the Seafox 2 is calculated from the hot spot stress ranges and the number of recorded stress cycles at each location in a governing critical joint. The analysis shows that when the Seafox 2 continues to operate in the North Sea, its un-factored design fatigue life is 262,2 years (87,4 years when a design fatigue factor is applied). It can, therefore, be concluded that the Seafox 2 will not fail due to metal fatigue in the North Sea operating environment in the near future.

Generally, scatterplots and wave spectra are used to predict future wave conditions and thus wave loading at a certain given location. These industry standards are accurate for fixed platforms but Jack-ups move around and thus encounter a larger variety of different environmental conditions. This study uses historical data on actual environmental conditions encounter by Seafox 2

When comparing the fatigue life of the Seafox 2 calculated in this study to the fatigue life calculated in 1983 a significant difference is found. Differences are also found in environmental input data which suggest the hindcasting method used in this thesis can attribute to a more comprehensive way for describing environmental loading for multiple locations. This method especially ads value when a Jack-up has operated in different locations.

The ultimate limit state for the Burj is calculated for three locations. Two are possible locations where the Burj might be deployed and one is a model benchmark. The Burj is modelled in the same manner as the Seafox 2. From the results it can be concluded that steel diminution has a considerable impact on the ultimate limit state. The Burj cannot operate anymore in deep waters. However, in shallow waters it can still operate safely. For operations in intermediate waters (e.g.the Al Shaheen field) further detailed structural analyses must be conducted. The analysis presented in this thesis shows that narrowing the work scope of the Burj to shallow waters is a viable way to avoid costly leg repairs.

10 Recommendation

The research presented in this thesis supports the following recommendations:

Simplifications have been made in modelling the environmental loads. Most of these simplifications were conservative ones. For a more accurate approach these simplifications have to be minimized. Due to the conservativeness of this analyses the conclusion on fatigue life only works one way. If results of this study had shown a fatigue life less than 30 years this would not mean the Seafox 2 could not operate anymore. In this case a less conservative analysis could be conducted.

In this thesis the Jack-up legs are assumed to have pinned supports. In reality the fixity of the supports lie somewhere in between fixed and pinned. The effect of fixity on the dynamic response needs further research.

This thesis concludes the Seafox 2 can rain operational and has no limit on However due to inherent uncertainties associated with a fatigue analyses and the simplifications made the analysis it is still recommended to check the legs for cracks around the splash zone and guide frames.

To conduct accurate fatigue analyses in the future, Seafox is recommended to keep accurate environmental data for all Jack-ups in all operating locations.

Generally, this study finds that diminution has substantial effect on fatigue life. This finding warrants further investigation of the cumulative effect of these processes. The work done to date and presented here has already contributed materially to a commercial decision by the Seafox organization to narrow the work scope of the Burj to shallower waters and thus avoid or, at least, delay costly leg repairs. However, detailed research is needed into the relation between steel diminution and fatigue life.

11 Bibliography

5-5A, S. (2008). *The Society of Naval Architects and Marine Engineers.* New Jersey.

Adams, N. B. (1991). *Dynamics of Fixed Marine Structures.* Butterworth Heinamann.

Collins, A. (1993). Failure Of Materials In Mechanical Design. John Wiley And Sons Ltd.

DNV-GL. (2015). *Environmental conditions and environmental loads.* Høvik, Norway: Det Norske Veritas.

DNVGL-RP-C203. (2016). *Fatigue design of offshore steel structures.* DNV GL AS.

DNVGL-RP-C210. (2015). *Probabilistic methods for planning of inspection for fatigue cracks in offshore structures.* DNV GL AS.

DNVGL-RU-OU-0104. (2015). *Rules for classification.* DNV-GL.

DNV-RP-C101. (2015). *Thickness Diminution for mobile offshore units.* DNV-GL.

HSE, L. R. (1997). *Stress concentration factors for simple tubular joints.* Norwich: HSE Books.

Hydrodynamics, U. (2010). *Theory description of use verification.* USFOS.

J.L. Humar, H. X. (1993). *Dynamic response analysis in the frequency domain.* Ottowa: Department of Civil Engineereng, Carleton University.

Nagtegaal, J. C. (1982). On the implementation of inelastic constitutive equations with special reference to large deformation problems. *Computer Methods in Applied Mechanics and Engineering*, 469 - 484.

NEN-EN-ISO, 1. (2012). *Petroleum and natural gas industries - Sitespecific assessment of mobile offshore units.* Delft: Nederlande Normailisatie instituut.

O. Weeger, U. W. (2013). *Nonlinear frequency response analysis of structural vibrations.* Kaiserslautern: TU Kaiserslautern, Faculty of Mathematics.

P.J. Knight M.J. Howarth D.F. Flatt and S.G. Loch. (1992). *Current profile an sea-bed prerssure and temperature records.* Merseyside: Proudman Oceanographic Labratory.

Paris P.C., e. F. (1963). A critical analysis of crack propagation laws. J Basic Eng.

Schutz, W. (1996). A history of fatigue. In *Engineering Fracture Mechanics* (pp. 263–300). Elsevier.

Singh, R. (2014). *Corrosion control for offshore structures.* Waltham, massachusetts: Gulf Professional Publishing.

Sobczyk K., S. J. (1992). *Random Fatigue: From Data to Theory.* Academic press Inc.

Tirant, P. L. (1993). *Stability and operation of jackups.* Paris: Editions Technip.

USFOS Manual. (n.d.). Retrieved from ufos.no: http://www.usfos.no/

USFOS Manual. (n.d.). Retrieved from ufos.no: http://www.usfos.no/